ETSI TR 102 311 V1.2.1 (2015-11)

TECHNICAL REPORT

Fixed Radio Systems;
Point-to-point equipment;
Specific aspects of the spatial frequency reuse method

Reference

RTR/ATTM-04029

Keywords

DFRS, digital, DRRS, FWA, MIMO, radio

ETSI

650 Route des Lucioles
F-06921 Sophia Antipolis Cedex - FRANCE

Tel.: +33 4 92 94 42 00   Fax: +33 4 93 65 47 16

Siret N° 348 623 562 00017 - NAF 742 C
Association à but non lucratif enregistrée à la
Sous-Préfecture de Grasse (06) N° 7803/88

Important notice

The present document can be downloaded from:
http://www.etsi.org/standards-search

The present document may be made available in electronic versions and/or in print. The content of any electronic and/or print versions of the present document shall not be modified without the prior written authorization of ETSI. In case of any existing or perceived difference in contents between such versions and/or in print, the only prevailing document is the print of the Portable Document Format (PDF) version kept on a specific network drive within ETSI Secretariat.

Users of the present document should be aware that the document may be subject to revision or change of status. Information on the current status of this and other ETSI documents is available at
http://portal.etsi.org/tb/status/status.asp

If you find errors in the present document, please send your comment to one of the following services:
https://portal.etsi.org/People/CommiteeSupportStaff.aspx

Copyright Notification

ETSI

Contents

Intellectual Property Rights

IPRs essential or potentially essential to the present document may have been declared to ETSI. The information pertaining to these essential IPRs, if any, is publicly available for **ETSI members and non-members**, and can be found in ETSI SR 000 314: *"Intellectual Property Rights (IPRs); Essential, or potentially Essential, IPRs notified to ETSI in respect of ETSI standards"*, which is available from the ETSI Secretariat. Latest updates are available on the ETSI Web server (http://ipr.etsi.org).

Pursuant to the ETSI IPR Policy, no investigation, including IPR searches, has been carried out by ETSI. No guarantee can be given as to the existence of other IPRs not referenced in ETSI SR 000 314 (or the updates on the ETSI Web server) which are, or may be, or may become, essential to the present document.

Foreword

This Technical Report (TR) has been produced by ETSI Technical Committee Access, Terminals, Transmission and Multiplexing (ATTM).

Modal verbs terminology

In the present document "**shall**", "**shall not**", "**should**", "**should not**", "**may**", "**need not**", "**will**", "**will not**", "**can**" and "**cannot**" are to be interpreted as described in clause 3.2 of the ETSI Drafting Rules (Verbal forms for the expression of provisions).

"**must**" and "**must not**" are **NOT** allowed in ETSI deliverables except when used in direct citation.

Introduction

It has been known for a long time that in order to improve theoretically the capacity of a given communication channel with maintaining the existing power at the transmitter and SNR at the receiver, the best solution is to dismantle the aggregate single channel into independent orthogonal sub-channels all using the same carrier frequency. To this theoretical improvement a considerable practical implementation can be added, given that with the distributing of payload among sub-channels the required order of the modulation scheme can be reduced. One example of exploiting this payload distribution method can be found in the existing "co-channel dual polarization" mode. With this implementation the aggregate payload is distributed between the both orthogonal independent sub-channels - the two perpendicular linear polarization carriers. The present document describes a new approach of orthogonalization , the spatial frequency re-use. As in the case of polarization, in order to perform the separation at the receiver, a special module should be incorporated - similar to the cross-polarization Interference Canceller (XPIC) - the Spatial Frequency Reuse Canceller (SFRC). In general, the SFR method is not limited to only two sub-channels as in the CCDP case, and systems that use it are able to double, triple or multiple the spectral efficiency without any trade off on the system gain as it is normally the case with improving the spectral efficiency by going to high order QAM modulation.

The present document includes an updated view of the SFR scheme using Multiple Antenna Techniques (MIMO). Furthermore, some theoretical aspect reviews, installation issues, results from a new in field trial, considerations about planning and, in the end, a living list for relevant standards modifications have been added.

Main changes reported in the present document are related to the MIMO system model, performance with non-optimal antenna spacings, installation issue, new field trial, antenna composite RPE and MIMO deployment status in Europe.

1 Scope

The present document provides, initially, a theoretical overview of how point-to-point systems that use SFRC could improve the link capacity and/or system gain, or could focus power in different directions or cover an area. Focus is put on LOS links.

In general these different results may "compete" with one another and for example an increase of capacity may require an increase of system gain. Few basic methods for implementing SFR are provided in the present document.

Simulation and field trial results are provided in order to show the discussed techniques and the main improvements for the SFRC over the "Internal" Co-Channel Interference (ICCI).

Main report subjects:

- Increase the link capacity (by increasing the spectral efficiency).

- Increase the link system gain (by increasing the receiver SNR).

- Methods of implementing SFR (by using MIMO).

- Verification by simulations and trials.

- Improvement parameter definition.

- Planning matters (installation issues and availability calculation).

- Living list for standard modifications.

2 References

2.1 Normative references

References are either specific (identified by date of publication and/or edition number or version number) or non-specific. For specific references, only the cited version applies. For non-specific references, the latest version of the reference document (including any amendments) applies.

Referenced documents which are not found to be publicly available in the expected location might be found at http://docbox.etsi.org/Reference.

NOTE: While any hyperlinks included in this clause were valid at the time of publication, ETSI cannot guarantee their long term validity.

The following referenced documents are necessary for the application of the present document.

Not applicable.

2.2 Informative references

References are either specific (identified by date of publication and/or edition number or version number) or non-specific. For specific references, only the cited version applies. For non-specific references, the latest version of the reference document (including any amendments) applies.

NOTE: While any hyperlinks included in this clause were valid at the time of publication, ETSI cannot guarantee their long term validity.

The following referenced documents are not necessary for the application of the present document but they assist the user with regard to a particular subject area.

[i.1] Recommendation ITU-R F.699: "Reference radiation patterns for fixed wireless system antennas for use in coordination studies and interference assessment in the frequency range from 100 MHz to about 70 GHz".

3   Definitions, symbols and abbreviations

3.1   Definitions

For the purposes of the present document, the following terms and definitions apply:

Eigenvalue (λ^2): Eigenvalues of the matrix $\mathbf{H} \times \mathbf{H^H}$ are the root of the characteristic equation:

$$\det(H \times H^H - \lambda^2 I) = 0$$

expectation (E_H): weighted average value of a Random Variable over all possible realizations that the Random Variable may assume

NOTE 1:   The weight coefficients are the probability value that the Random Variable assumes that value.

NOTE 2:   Subscript "**H**" refers to the name of the Random Variable, for the reference scope "**H**" is the Channel Matrix.

EXAMPLE: Mathematical formulation:

- **discrete scalar random variable "X":** "X" takes values "x_1, x_2…" with probabilities "p_1, p_2…"

$$E[X] = \sum_{i=1}^{\infty} x_i \times p_i$$

- **continuous scalar random variable "X":** "X" takes continuous values and $f(x)$ is the probability density function

$$E[X] = \int_{-\infty}^{+\infty} x \times f(x) \cdot dx$$

- Matrix Random Variable "H":

$$E_H[H_{NM}] = E\begin{bmatrix} h_{11} & h_{12} & ... & ... & h_{1M} \\ h_{21} & h_{22} & ... & ... & h_{2M} \\ ... & ... & ... & ... & ... \\ ... & ... & ... & ... & ... \\ h_{N1} & h_{N2} & ... & ... & h_{NM} \end{bmatrix} =$$

$$= \begin{bmatrix} E[h_{11}] & E[h_{12}] & ... & ... & E[h_{1M}] \\ E[h_{21}] & E[h_{22}] & ... & ... & E[h_{2M}] \\ ... & ... & ... & ... & ... \\ ... & ... & ... & ... & ... \\ E[h_{N1}] & E[h_{N2}] & ... & ... & E[h_{NM}] \end{bmatrix}$$

Hadamard product ($\circ$): operation that takes two matrices of the same dimensions, and produces another matrix where each element "ij" is the product of elements "ij" of the original two matrices

Hermitian transpose ($\cdot)^H$: N $\times$ M matrix "**H**" with complex entries is the M $\times$ N "**H***" matrix obtained from "**H**" by taking the transpose and then taking the complex conjugate of each matrix entries

NOTE: Also known as Complex Transpose.

matrix trace (Tr): trace of an N × N square matrix "**Q**" is defined to be the sum of the elements on the main diagonal

$$Tr(Q) = q_{11} + q_{22} + \ldots q_{NN} = \sum_{i=1}^{N} q_{ii} = \sum_{i=1}^{N} \lambda_i$$

power constraint: constraint applicable to the total transmission power level of the MIMO system (P_{MIMO}) with respect to the transmitted power level by the SISO system (P_{SISO})

NOTE: If the MIMO system transmits the same power level of the reference SISO system then the power constraint holds. Otherwise if P_{MIMO} is higher than P_{SISO}, e.g. in case of N × M MIMO → $P_{MIMO} = N \times P_{SISO}$, the constraint does not hold.

singular value (λ): defined as the square root of the Eigenvalues

3.2 Symbols

For the purposes of the present document, the following symbols apply:

α	Transmission Power Weight (for Water Filling/Pouring)
A	Free Space Loss and Fading Attenuation Effects Matrix
argmin(.)	Argument which minimize the brackets content
B	Bandwidth
C	Capacity [bit/s/Hz]
dB	decibel
dBc	decibel relative to mean carrier power
dBi	decibel relative to an isotropic radiator
dBm	decibel relative to 1 milliWatt
dBW	decibel relative to 1 Watt
d_{opt}	Optimal Distance between Antennas
E_H	Expectation over variable H
H	NxM Channel Matrix
I	Unitary Matrix
λ	Singular Value of Channel Matrix (**H**)
$λ^2$	Eigenvalue of Matrix $\mathbf{H} \cdot \mathbf{H}^H$
M	Number of Transmit Antennas
m	Modulation Order
N	Number of Receive Antennas
N_0	Noise Power Spectral Density
P	Transmission Power Level
P_{MIMO}	Transmission Power Level of MIMO system (total)
P_{SISO}	Transmission Power Level of SISO system
ppm	parts per million
ρ	SNR
$\overline{S}$	Average Received Power
X	Polarization Effects Matrix (XPD)
det	Matrix Determinant
Tr	Matrix Trace
∘	Hadamard Product
|·|	Absolute Value
$(\cdot)^H$	Hermitian Transpose

3.3 Abbreviations

For the purposes of the present document, the following abbreviations apply:

AWGN	Added White Gaussian Noise
BER	Bit Error Ratio
BLAST	Bell Laboratories Layered Space Time
C/N	Carrier to Noise
CCDP	Co-Channel Dual Polarization
CEPT	Comité Européen des Postes et Télécommunications
CS	Channel Separation

CTF	Channel Transfer Function
ECC	Electronic Communication Committee
FS	Fixed Service
ICCI	"Internal" Co-Channel Interference
IDU	InDoor Unit
ITU-R	International Telecommunication Union - Radiocommunication
LOS	Line Of Sight
MIMO	Multiple Input Multiple Output
ML	Maximum-Likelihood
MMSE	Minimum Mean Square Error
MP	Multi-Path
MSE	Mean Square Error
MW	MicroWave
nLOS	near-Line Of Sight
NLOS	Non-Line Of Sight
PP	Point-to-Point
PTP	Point To Point
QAM	Quadrature Amplitude Modulation
RF	Radio Frequency
RIC	Radio Interface Capacity
RPE	Radiation Power Envelope
RSL	Received Strength Level
Rx	Receiver
SAW	Surface Acoustic Wave
SDG	Spatial Diversity Gain
SFR	Spatial Frequency Re-use
SFRC	Spatial Frequency Reuse Canceller
SISO	Single Input Single Output
SNR	Signal to Noise Ratio
STD	Standard Deviation
SVD	Singular Value Decomposition
T	Symbol Period
Tx	Transmitter
UCA	Uniform Circular Array of antenna
ULA	Uniform Linear Array of antenna
URA	Uniform Rectangular Array of antenna
VBLAST	Vertical Bell Laboratories Layered Space Time
XPD	Cross-Polarization Discrimination
XPIC	Cross-Polarization Interference Canceller
ZF	Zero-Forcing

4 Overview

4.1 Capacity improvement of the MIMO system (Spatial Multiplexing)

For an $N \times N$ MIMO systems the "Spatial Multiplexing" refers to the promising Capacity improvement. Basically, "N" independent orthogonal sub-channels, are provided on the same communication channel (CS), then the SISO maximal achievable spectral efficiency (C) is multiplied by a factor "N" without adding any power resource (i.e. for the MIMO system the single transmitter level is P/N). Figure 4.1 shows a Single Input Single Output (SISO) system compared with a Multiple Input Multiple Output (MIMO) using the same physical resource i.e. the given channel (CS).

This is valid only in some conditions: when the sub-channels are orthogonal or independent which means that the statistical expectation of the product of samples of the signals taken from any pair of the independent sub-channel is very low or ideally null.

For the purpose of such capacity improvement any orthogonalization method is valid, either polar or spatial. In addition to the theoretical capacity improvement there is also the available practical improvement. In practice the division of the aggregate payload among the sub-channels facilitates lowering the order of the modulation. For example, aggregate capacity of 156 Mbit/s over 28 MHz, when divided between two sub-channels, each one of them carrying only 78 Mbit/s over 28 MHz channel. In comparison, a single channel payload implementation requires 128 QAM constellations, while with the sub-channel approach a 16 QAM per carrier is sufficient. From the equations in figure 4.1 it can be concluded that the theoretical difference between the two approaches is 9 dB, however due to practical considerations such as linearity and phase noise, the gain improvement is higher, i.e. around 11 dB.

$$C \propto log_2 \ (SNR)$$

$$C \propto N \log_2 (SNR)$$
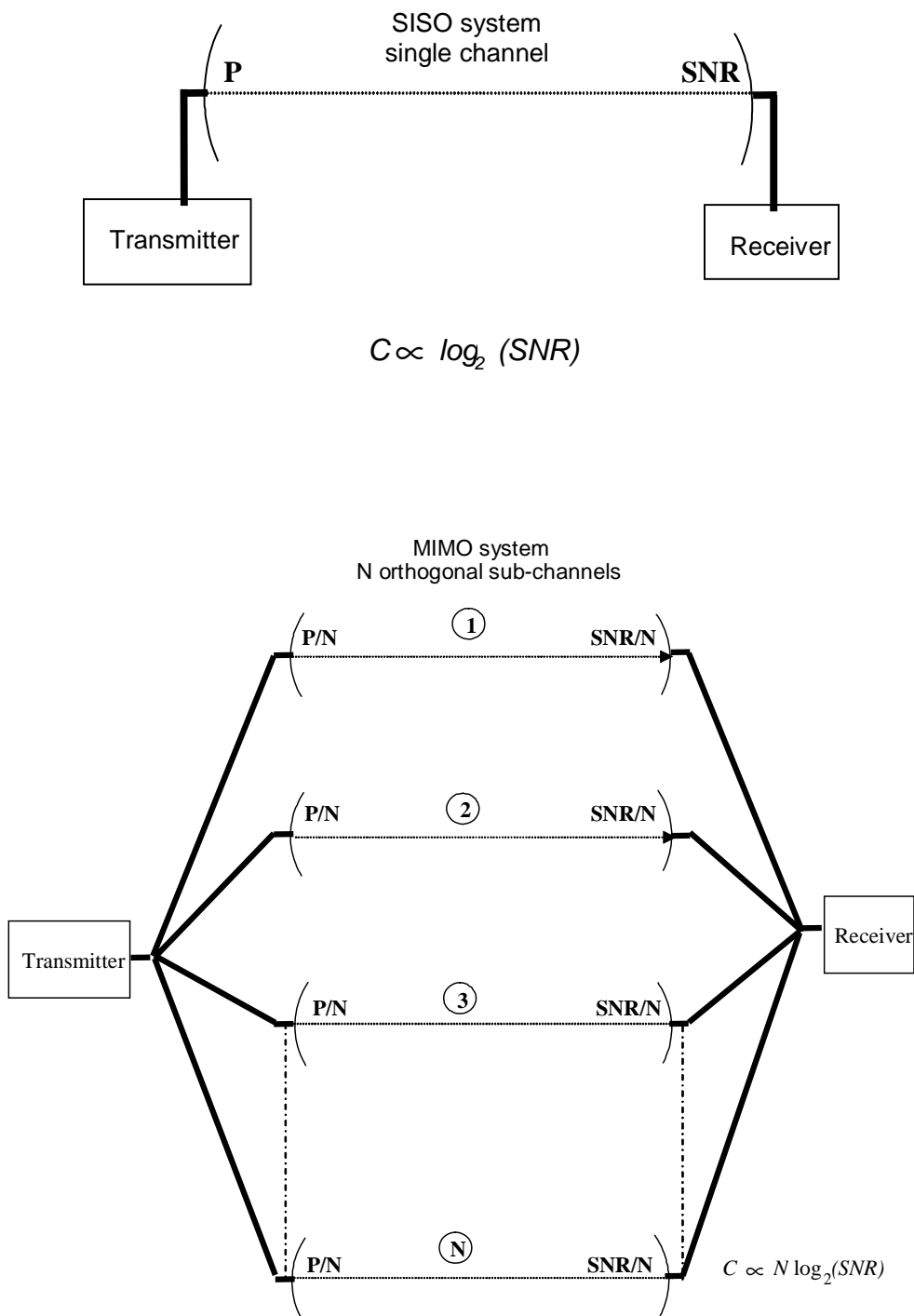
Figure 4.1: Comparison between SISO system and MIMO system

4.2   Difference between Cross-Polarization and Spatial Frequency Reuse (MIMO)

Unlike from the cross-polarization case, e.g. used in CCDP systems, where the Cross Polarization Discrimination (XPD) in "normal" conditions limits that the energy of one polarization signal falls back into the other polarization status, in a spatial frequency reuse system the energy of all sub-channels are at similar levels and all mixed together creating a lot of mutual interference between sub-channels.

Figure 4.2 compares the receiving sections of a cross-polarization system against spatial frequency reuse system (2×2 MIMO). The meanings of the variables in the figure 4.2 are:

- r^i_{xi} : received signal component at antenna element i-th (i = 1, 2) generated by the transmitted signal x_i.

- y^i_{xi} : i-th (i = 1, 2) demodulated signal component generated by transmitted signal x_i and received at antenna element i-th (i = 1, 2).

- r^i : the whole received signal at antenna element i-th (i.e. $r^1 = r^1_{x1} + r^1_{x2}$ and $r^2 = r^2_{x1} + r^2_{x2}$).

- y^i : the whole demodulated signal from antenna element i-th (i.e. $y^1 = y^1_{x1} + y^1_{x2}$ and $y^1 = y^1_{x1} + y^1_{x2}$).

Thus two cases arise:

1)   Cross-Polarization System

In this system two antennas, one for each polarization status (e.g. horizontal and vertical) are present.

In an ideal case without any cause of depolarization, e.g. the antenna XPD is high enough and no rain or other atmospheric phenomena are active, at V-polarized antenna (i = 1) the received signal power level of the V-polarized transmitted signal (r^1_{x1}) is much higher than the received signal power level of the H-polarized transmitted signal (r^1_{x2}). The same stands with inversed behaviour between the polarization status signals for the second antenna (i = 2).

XPIC algorithm cancels the self-interference of the unwanted polarization signal, for example H for the first antenna and V for the second one.

2)   Spatial Frequency Reuse (MIMO) System

Even in this system two antennas, or more, are present but they may use the same polarization (in the example the vertical one).

In this case the received signal components, the couple (r^1_{x1}, r^1_{x2}) for antenna 1 and (r^2_{x1}, r^2_{x2}) for antenna 2, at each antenna have similar power level and the received signal components are not orthogonal to each other. Thus the difference in the phase of the signals, due to different sub-channel paths (space diversity), generated by MIMO antenna arrangement forms a kind of "orthogonality" or diversity between y^1 and y^2.

An SFRC algorithm can facilitate the separation of the mixed input signals for data detection and, as well, the cancellation of the generated self-interference preventing any degradation on the received threshold.

NOTE: Orthogonality between two signals can be defined as a zero expectation of their sampled product over the symbol period T.

Spatial Frequency Reuse and Cross-Polarization may be exploited together in order to increase the number of independent sub-channels (Multi-Polarized MIMO).
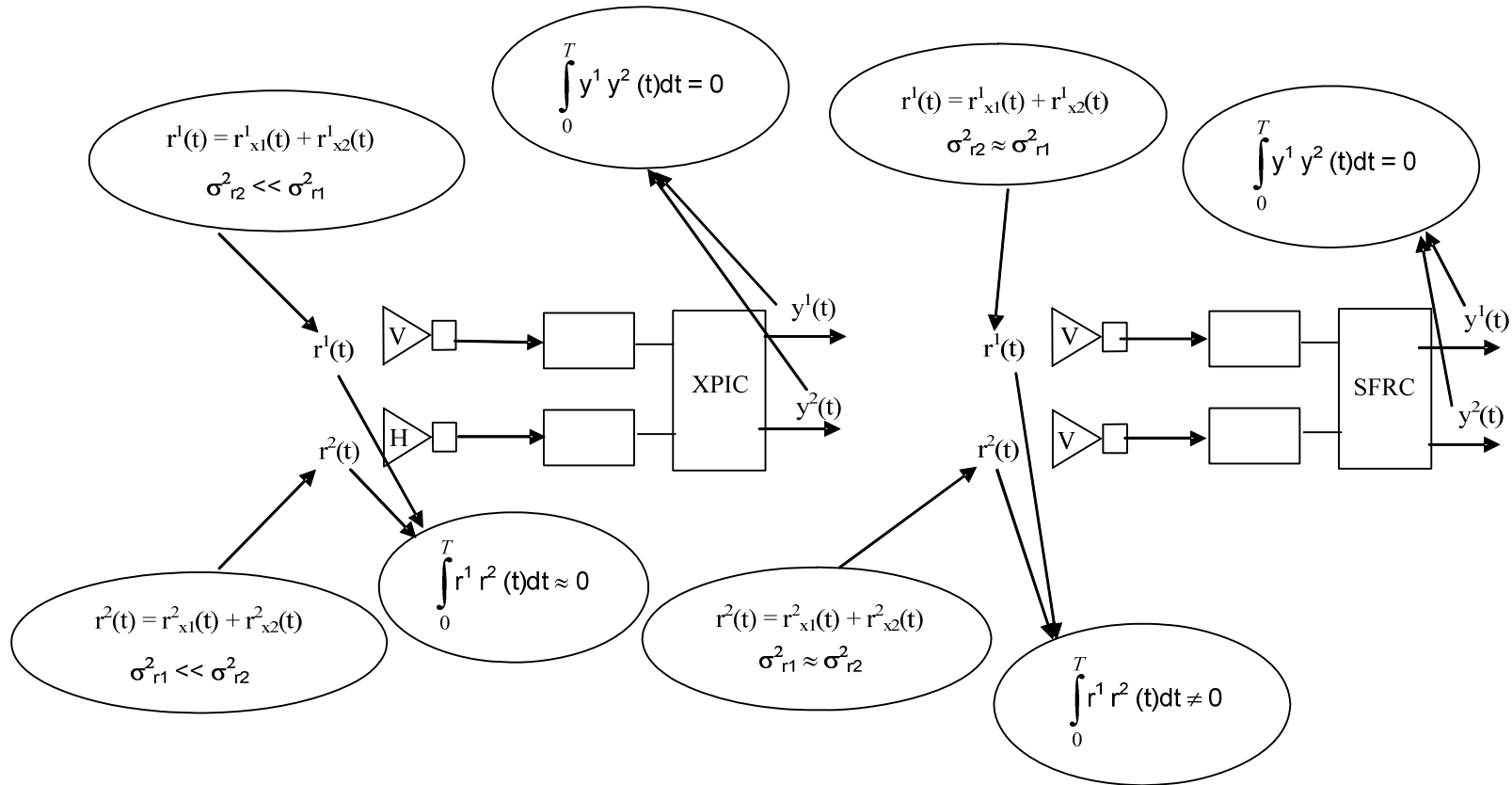
Figure 4.2: Cross-polarization versus spatial frequency reuse

4.3   Methods to achieve spatial frequency reuse

4.3.1   Spatial configuration

4.3.1.1   MIMO channel with spatial configuration

Figure 4.3.1.1 describes a typical communication channel with spatial configuration which also stands for spatial frequency reuse applications. In the example three antennas are considered either in transmission and receiver sides, thus it can be defined as a 3×3 MIMO system.

The dotted lines in figure 4.3.1.1 represent the sub-channels between each couple of transmit and receive antennas. Mathematically the coefficients "h_{ij}" (i, j = 1…3) denote the Channel Transfer Function (CTF) and all together the coefficients form a Channel Matrix" **H**". The received signal at each antenna port is a linear combination of the transmitted signals (see clause 4.2 and figure 4.2).
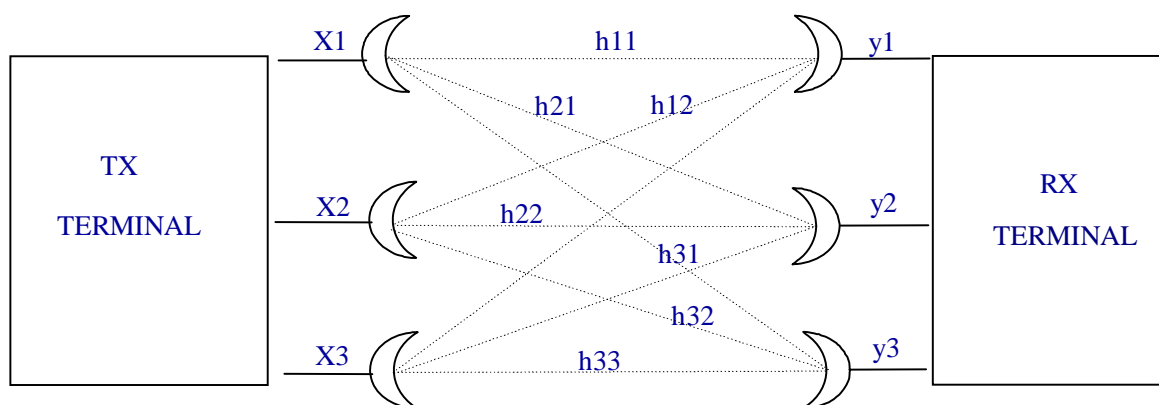
Figure 4.3.1.1: 3 × 3 MIMO channel with spatial configuration

4.3.1.2   MIMO System Model

In figure 4.3.1.2 it is depicted a MIMO System Model block diagram. The meaning of the symbols follows:

  X   = TX symbol vector

  x_j = j-th input signal at j-th transmit antenna

  R   = received signal vector

  r_i = i-th received signal at i-th receive antenna

  Y   = RX estimated symbol vector

  y_i = i-th output signal at i-th receive antenna

  H   = Channel Matrix

  h_{ij} = Channel Transfer Function coefficient from antenna 'j' (TX) to antenna 'i' (RX)

  N   = Noise signal vector

  n_i = i-th noise signal at i-th receive antenna
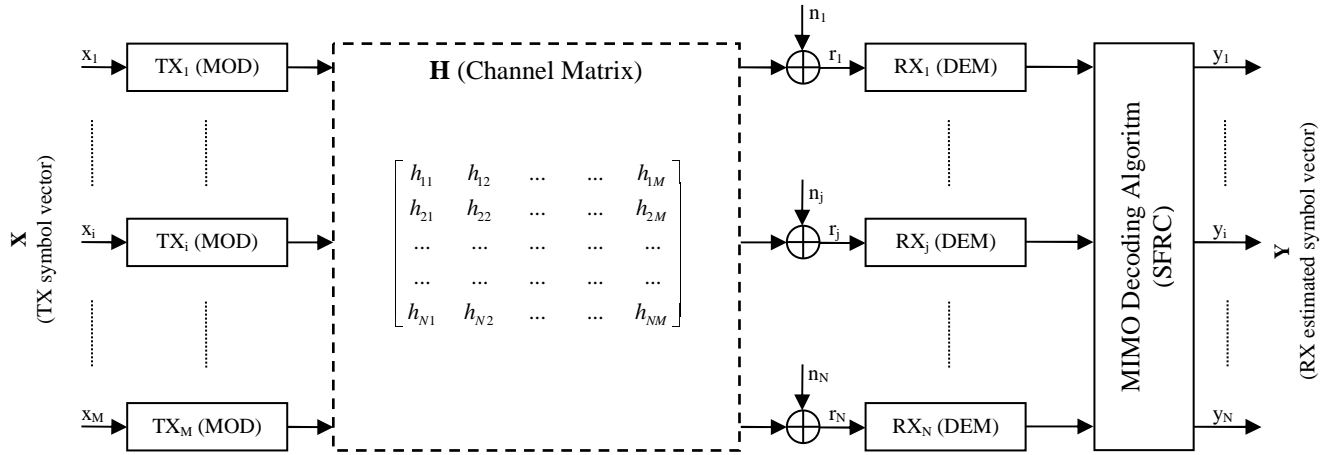
Figure 4.3.1.2: MIMO System Model

In general, the channel coefficients can be represented as a complex value:

$$h_{ij} = \alpha_{ij}(f)\, e^{\,j\beta ij(f)}$$

where:

"$\alpha_{ij}(f)$" is the attenuation characteristic of the (i, j) sub-channel (as a function of the frequency)

"$\beta_{ij}(f)$" is the phase characteristic of the (i, j) sub-channel (as a function of the frequency)

Under above defined assumptions ($\mathbf{I} = M \times N$ pseudo-identity matrix):

$$\mathbf{Y} = \mathbf{H} \times \mathbf{X} + \mathbf{I} \times \mathbf{N} \rightarrow y_i = \Sigma_j\,(h_{ij}\,x_j) + n_i \text{ with } j = 1\ldots M$$

NOTE 1: $\mathbf{I}$ is a M x N pseudo-identity matrix.

NOTE 2: The model is depicted only in one direction but in real situation the link may be bi-directional.

In RX side the core of the MIMO Decoding Algorithm is the estimation of the channel matrix and the computation of the inverse matrix "$\mathbf{H^{-1}}$" (i.e. $\mathbf{H} \cdot \mathbf{H^{-1}} = \mathbf{I}$). The above defined assumption results in:

$$\mathbf{Y} = \mathbf{H^{-1}} \times \mathbf{R} = \mathbf{H^{-1}} \times (\mathbf{H} \times \mathbf{X} + \mathbf{I} \times \mathbf{N}) = \mathbf{I} \times \mathbf{X} + \mathbf{H^{-1}} \times \mathbf{N} \rightarrow y_i = x_i + \Sigma_j\,(h^{-1}{}_{ij}\,n_i)$$

In order to obtain "$\mathbf{H^{-1}}$", the coefficients of the channel matrix, "$\mathbf{H}$" are necessary. In other words, an estimation of the channel parameters, "$\alpha_{ij}(f)$" and "$\beta_{ij}(f)$", is required. This operation is usually named "Channel Estimation".

4.3.2 Spatial frequency reuse based on rich scattering

This method of achieving orthogonality is valid when the link path has considerable amount of multipath scattering caused by reflections and diffractions on obstacles. This scenario is common in the lower frequency, usually below 6 GHz, where often application scenarios do not present direct line of sight connections. Figure 4.3.2 describes such a link. The multipath scattering provides statistical independent paths for the signals which reach the receiver with different amplitude, phase and delay attributes.
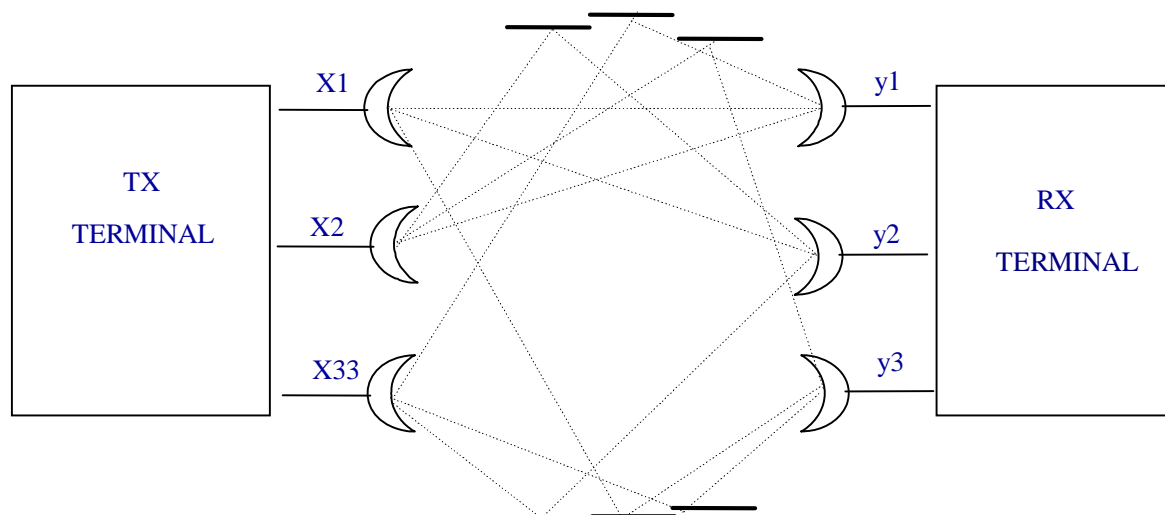
Figure 4.3.2: Spatial system scattering based

Mathematically in this system with sufficient diversity the elements of the channel matrix (**H**) become independent and identically distributed (i.i.d.) circular complex Gaussian terms. When **H** elements approaching this condition **H** becomes "high rank" and "more" orthogonal, and its singular values spread drops.

Such a system has the advantage that it has not great dependency on the antenna geometry, in contrast to the case described in next clause, as lower spacing between the antennas in the array is sufficient to get diversity between sub-channels (in the order of 5 or 10 times the wavelength).

However there is great disadvantage with these systems as they are based on scattering due to nLOS/NLOS propagation, large propagation attenuation should be taken into account when planning the system link budget. This is a fact that, with the variability of the channel conditions, causes the capacity to be statistical variable.

This scheme is addressable more by WiFi™ and access radio systems where usually there may be no line of sight signal components.

NOTE 1: If the line of sight component exists, it increases the dependency between sub-channels, reducing the rank of the matrix, and reduces the orthogonality between sub-channel paths.

NOTE 2: Wifi™ is an example of a suitable product available commercially. This information is given for the convenience of users of the present document and does not constitute an endorsement by ETSI of this product.

4.3.3 Spatial frequency reuse based on link geometry

4.3.3.1 Channel matrix pure line of sight case

Consider a MIMO system with N transmit antennas and M receive antennas. Figure 4.3.3.1a describes the case of M = N = 2 antennas at TX and RX sides where the antenna arrays are formed by parallel and equally spaced elements.

The path length difference between adjacent receive antennas (ΔR) is:

$$\Delta R = \sqrt{R^2 + d^2} - R \cong \frac{d}{2R}\left[\text{m}\right]$$

Where R is the link hop distance and d is the inter antenna element distance and the last approximation stands when R >> d.
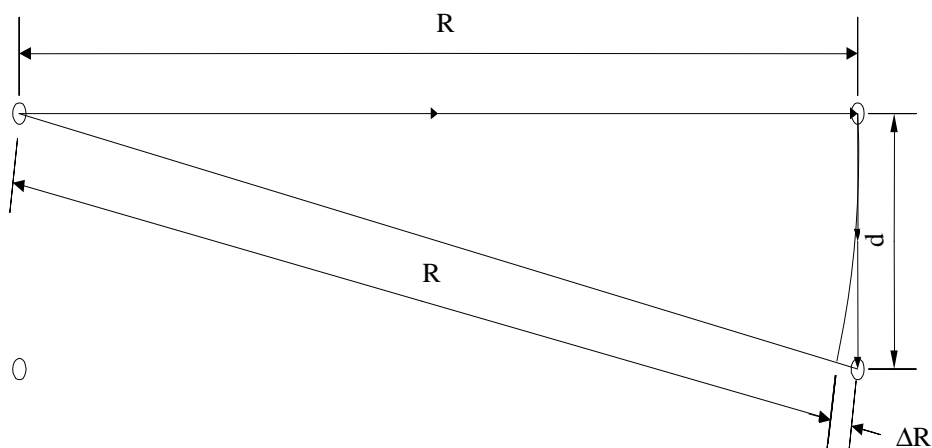
Figure 4.3.3.1.a: Differential path range in carrier propagation

The correspondent phase difference between two different paths is:

$$\varphi = \frac{2\pi}{\lambda}\Delta R \cong \frac{\pi}{\lambda}\times\frac{d^2}{R} \quad \text{[rad]}$$

where $\lambda = c / f$ is the wavelength of the used carrier.

Thus for the 2×2 MIMO as in figure 4.3.3.1.b the channel matrix becomes:

$$[H] = \begin{bmatrix} 1 & e^{j\phi} \\ e^{j\phi} & 1 \end{bmatrix}$$
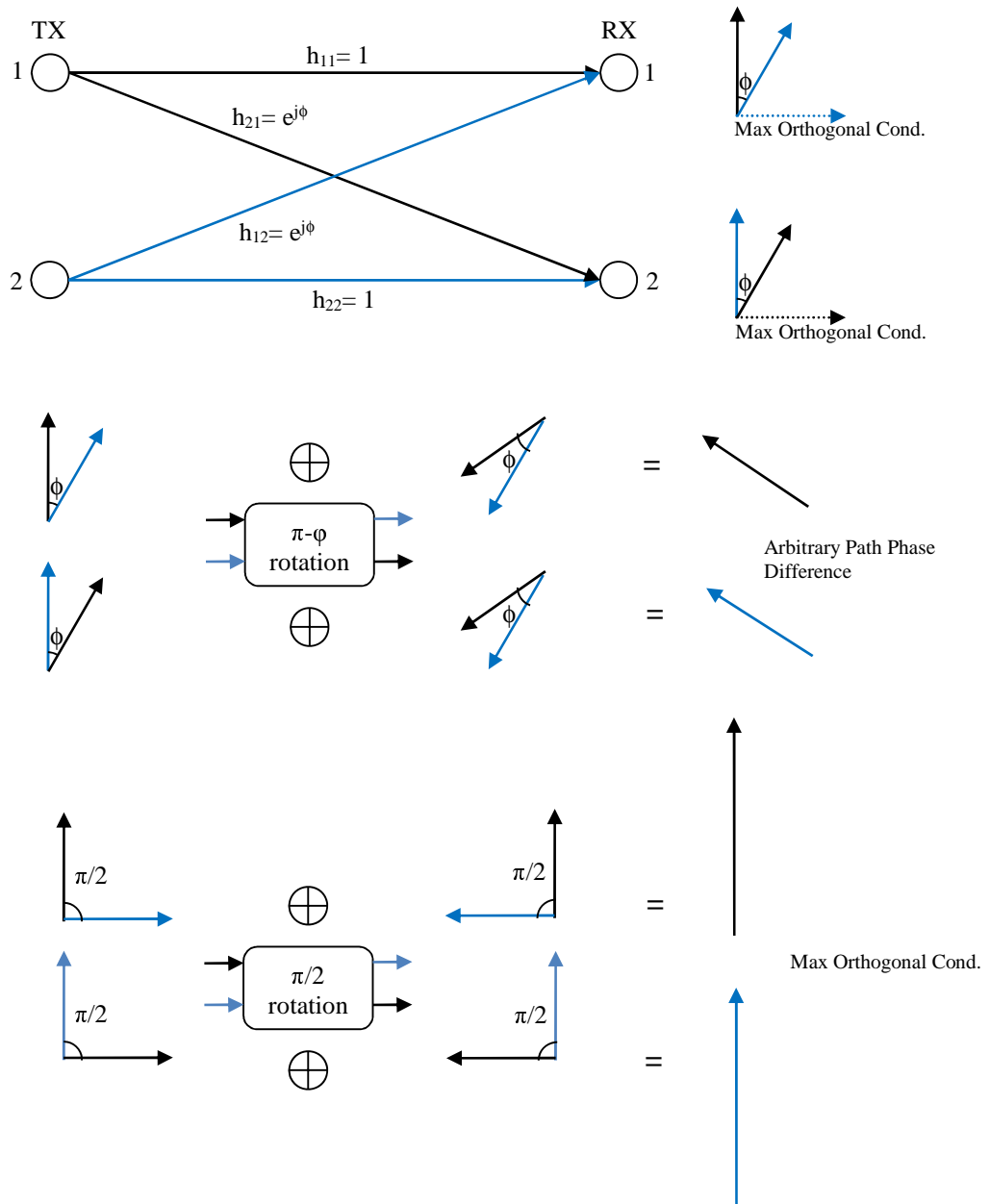
Figure 4.3.3.1.b: Vector Visualization

Instead for a 4×4 MIMO system **H** becomes:

$$[H] = \begin{bmatrix} 1 & e^{j\phi} & e^{j4\phi} & e^{j9\phi} \\ e^{j\phi} & 1 & e^{j\phi} & e^{j4\phi} \\ e^{j4\phi} & e^{-j\phi} & 1 & e^{j\phi} \\ e^{j9\phi} & e^{j4\phi} & e^{j\phi} & 1 \end{bmatrix}$$

And more in general for an N × N MIMO system:

$$[H] = \begin{bmatrix} 1 & e^{j\phi} & e^{j4\phi} & ... & e^{j(N-1)^2\phi} \\ e^{j\phi} & 1 & e^{j\phi} & ... & e^{j(N-2)^2\phi} \\ e^{j4\phi} & e^{j\phi} & 1 & ... & e^{j(N-3)^2\phi} \\ ... & ... & ... & ... & .... \\ e^{j(N-1)^2\phi} & & & & 1 \end{bmatrix}$$

4.3.3.2 Maximal orthogonal condition and optimal antenna spacing

In the channel matrix the columns correspond to the sub-channels from transmit antenna to all receive antenna, thus the mutual correlation calculated between the channel matrix columns correspond to the degree of "orthogonality" between the MIMO sub-channels. It is proofed by theory that the correlation is proportional to the quantity "$sin(N \cdot \phi)$" for an N × N MIMO system.

The sub-channels are independent if the result of the correlations between the sub-channels is null. This condition is equivalent to the statements:

$$\phi = \pm\pi / N + 2k\pi \text{ , k is any natural number}$$

These special points can be regarded as "the maximal orthogonal condition".

The "maximal orthogonal condition" can be depicted in the figure 4.3.3.2.a and 4.3.3.2.b as the point where the singular values of the 2 × 2 and 4 × 4 MIMO take the same value in function of the phase difference between the paths (φ). In practical situation the lower solution of φ for the maximal orthogonal condition is in the actual interest.
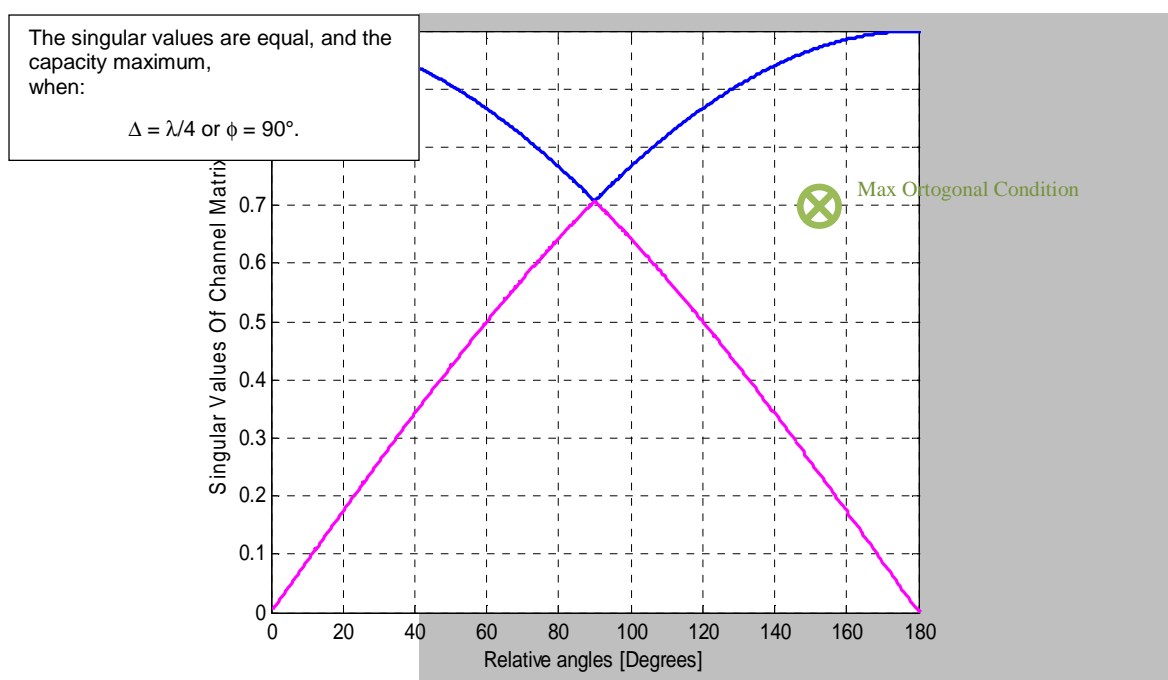
Figure 4.3.3.2.a: Orthogonal condition points 2 × 2 MIMO (normalized channel energy)

The singular values are equal, and the capacity maximum, when:

$\Delta = \lambda/8$ or $\phi = 45°$.

The corresponding antenna spacing is then:

$s^2 = r\lambda/4$.

For f = 28 GHz,
       r = 5 km,
       s = 3,6 m.
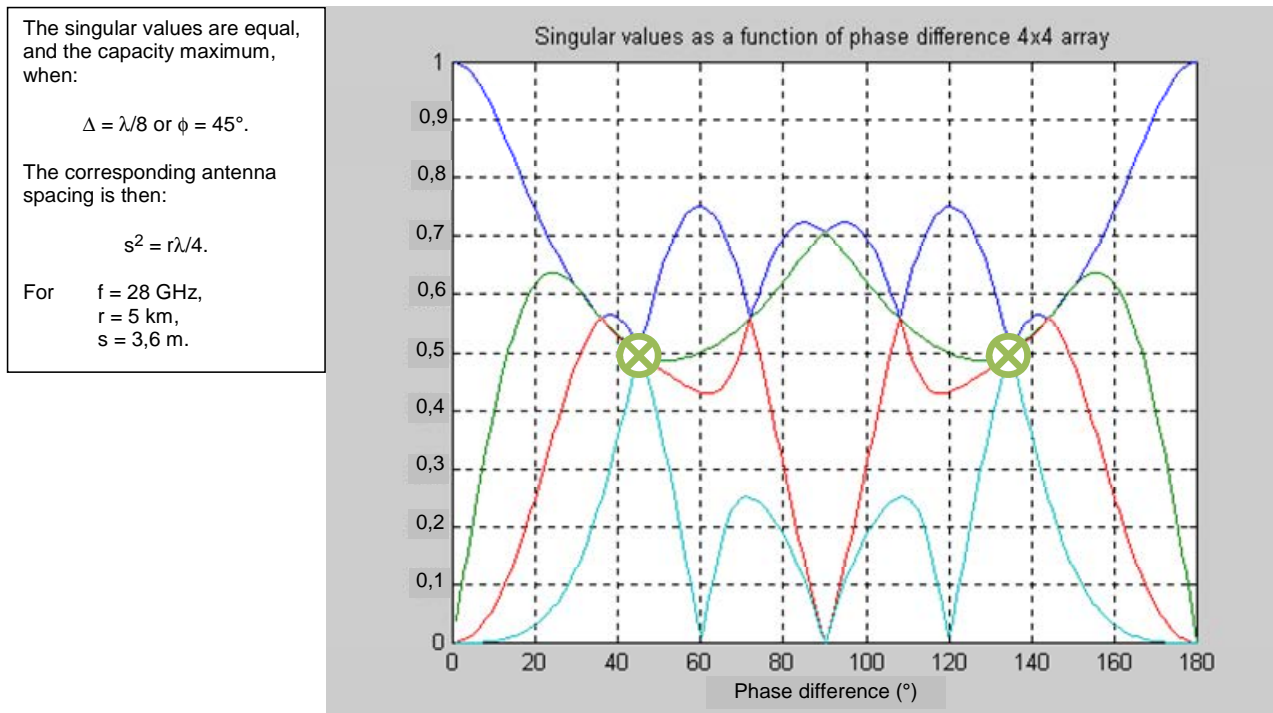
Figure 4.3.3.2.b: Orthogonal condition points 4 × 4 MIMO (normalized channel matrix)

It is of practical interest of finding the antenna spacing d_{opt} for the maximal orthogonal condition as function of the link hop distance (R), radio wavelength (λ) and the number of antennas (N):

$$d_{opt} = \sqrt{\frac{\lambda \times R}{N}}$$

$$[m] = \sqrt{\frac{[m][m]}{[no\_dimension]}} = \sqrt{[m^2]}$$

Above formula stands in case of the antenna separation is the same at both sides of the link and when the number of transmit antennas and receive antennas are the same (M = N).

More general formulation for optimal antenna spacing's at both link sides is:

$$d_1 \cdot d_2 = \frac{\lambda \times R}{\min(N, M)}$$

$$[m] \cdot [m] = \frac{[m][m]}{[no\_dimension]} = [m^2]$$

Where d_1 and d_2 are the antenna spacing values respectively at link edge 1 and link edge 2.

In figure 4.3.3.2.c the required antenna spacings dependence on link frequency and hop distance for the case of dual antenna array (2 × 2) are depicted for the 18 GHz, 23 GHz, 26 GHz, 28 GHz and 38 GHz frequency bands.
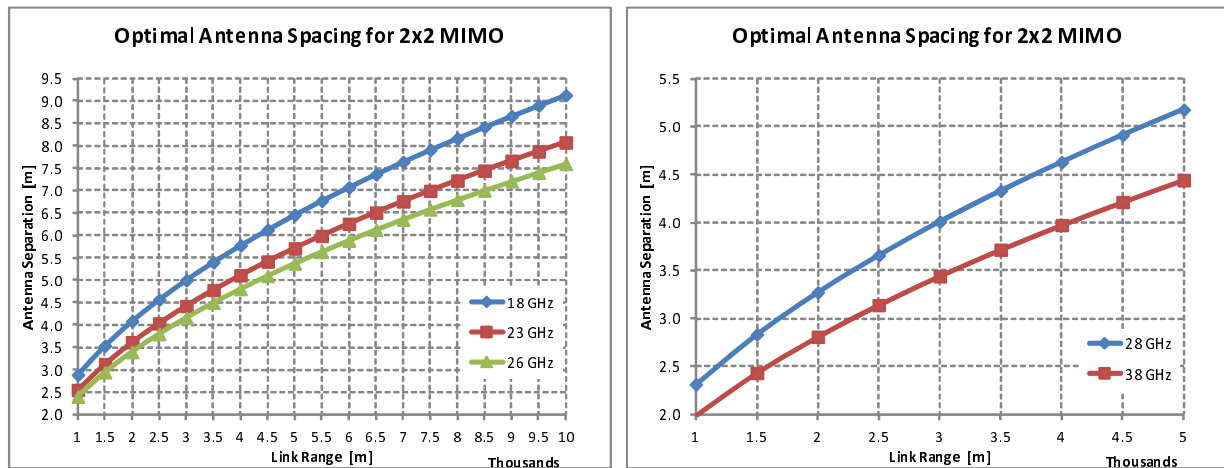
Figure 4.3.3.2.c: Antenna spacing for maximal orthogonal case

4.3.3.3 Spatial diversity gain

In general MIMO system can achieve both separation of independent input signals, that share the same frequency, and Spatial Diversity Gain (SDG) to the receiver over Single Input Single Output system (SISO), this gain is inherent to the system due to the antenna plurality.

The SDG value can easily be computed from the singular values λ of **H**. In the maximal orthogonal condition each singular value will be equal to SQRT(N) and the SDG value is equal to $10 \times \log_{10}$ (N).

4.3.3.4 Working with antenna spacing below the sub-optimal condition

Figure 4.3.3.4.a illustrates the singular values/SDGs of the two spatial channels in 23 GHz of 5 km hop distance for a 2×2 MIMO system. From figure 4.3.3.4.a it can be viewed that moving from optimal antenna spacing may cause only degradation in performance. As an example it can be seen from the diagram that 5,7 m is the antenna spacing that correspond to the maximal orthogonal condition SDG = $10 \times \log_{10}$ (2) (SDG = $10 \times \log_{10}$ (2) = 3 dB). If the antenna spacing will be reduced to 4,7 m one of the spatial channel will drop to 0 dB (same gain as a SISO reference system). Lowering the antenna spacing to 3,7 m degrades the weaker spatial channel by 3 dB compared to the SISO channel.

nt = 2 nr = 2 gamma = 0 f = 23 GHz h = 15 m D = 5 000 m Orient: VV dmax = 5,7 m
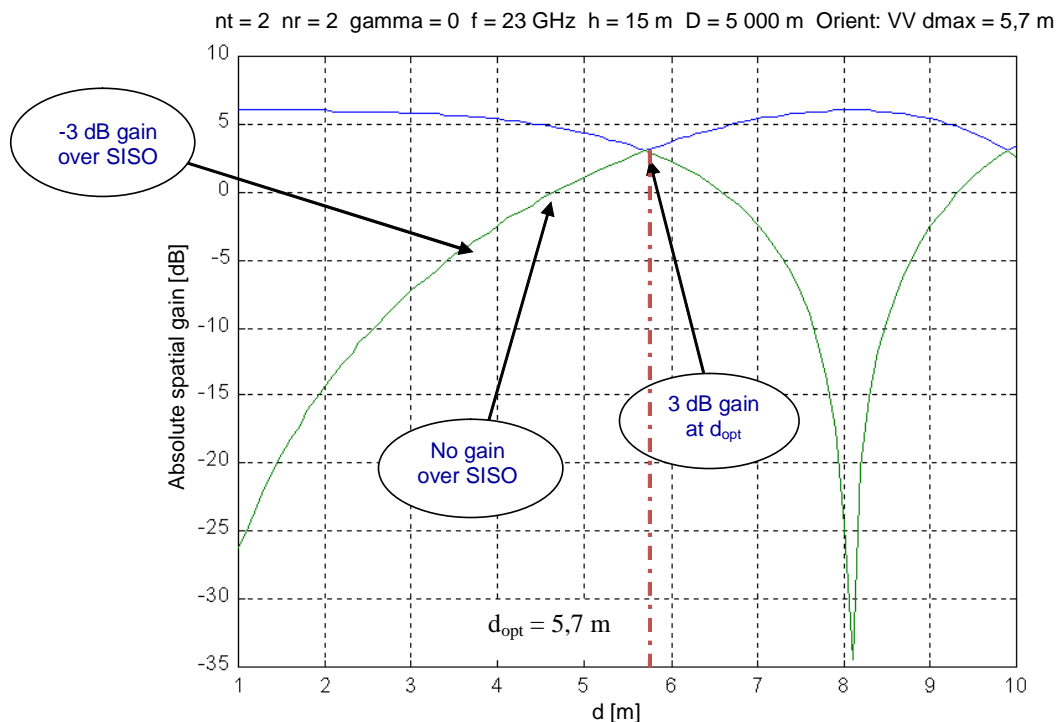
Figure 4.3.3.4.a: 2 × 2 MIMO spatial gain

For comparison in figure 4.3.3.4.b the singular values for 2×2 MIMO are reported in the case of considering the whole power level for the MIMO the same of the SISO one (sum power constraint), in the left, and without power constraint (doubling the SISO power level), in the right.

In case of the power constraint stands even in the optimal antenna spacing condition there is no SDG over the SISO case.
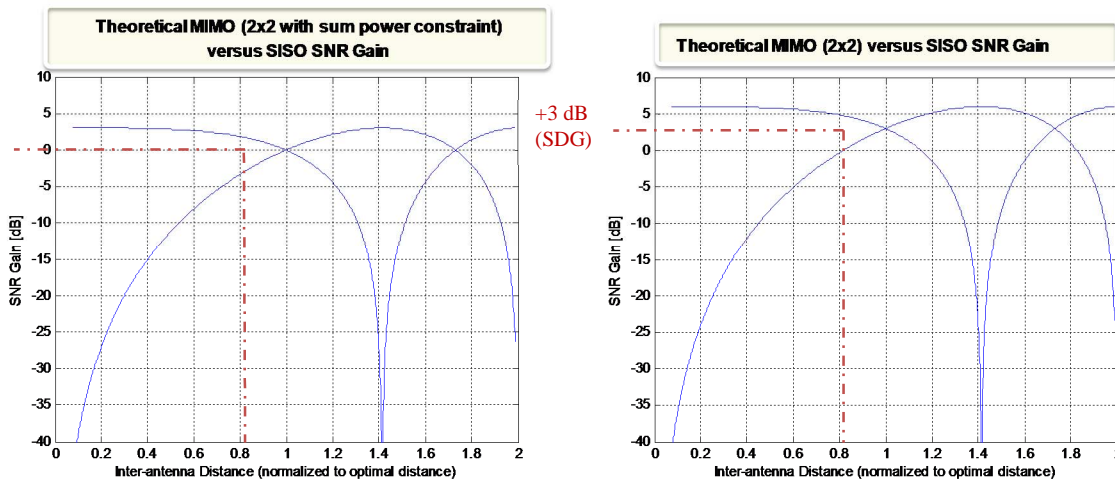
Figure 4.3.3.4.b: 2 × 2 MIMO spatial gain with and without sum power constraint

4.3.3.5   Channel matrix considering link propagation

In real link also propagation effects need to be considered. This is important in order to determinate the MIMO link performance, as it will be seen in term of Capacity in clause 4.4.

In practise even the path loss attenuation and any fading attenuation effects need to be accounted for any MIMO sub-channel. It is important to note that even in perfect propagation conditions, each sub-channel experiments different attenuation values due to difference in path distance. Such asymmetry behaviour is increased in working conditions due to even small activity in propagation fading, tolerance in transmission power level and receiver noise figure, antenna gains and geometric link misalignments.

The channel matrix **H** can be modified in a new matrix **H$_f$** as in the following:

$$H_f = |A| \circ H$$

where:

A = Free Space Loss and Fading Attenuation Effects Matrix (each elements represent the attenuation of the single sub-channel)

$|\cdot|$ = Matrix Single Element Absolute Value

$\circ$ = Hadamard Product

4.3.3.6 Multi-polarized MIMO

In a MIMO system also the two different polarizations, horizontal and vertical ones, may be used in order to create diversity. Furthermore, Multi-polarized MIMO can help to increase the number of sub-channels without increasing the total number of antenna by using dual polarized antenna. This is also important to save physical space for antenna array installation (e.g. 4×4 MIMO requires the installation of four antennas while a 2×2 Multi-Polarized MIMO requires just two dual-polarized antennas).

As in the previous clause, the channel matrix **H** can be modified in a new matrix **H$_x$** which take into account the polarization effects:

$$H_x = |X| \circ H$$

Where:

X = Polarization Effect Matrix (the elements are related to the XPD between the transmission and receive antenna couple)

4.4 MIMO Performance

In order to show MIMO Capacity improvement it is necessary to recall SISO Capacity limit. It is the famous Shannon-Hartley Theorem which states that the Capacity is:

$$C_{SISO} = \log_2(1+\rho) \ [\text{bit/s/Hz}]$$

Where:

$$\rho = \frac{\bar{S}}{N_0 \cdot B} = \text{SNR}$$

$\bar{S}$ = Averaged received Power [W]

N_0 = Noise Power Spectral Density [W/Hz]

B = Bandwidth [Hz]

NOTE: This formulation of the Shannon-Hartley Theorem stands for AWGN channel and Nyquist pulse shaping.

Following the MIMO model previously described in clause 4.3.1.2, it can be shown that the best performance which could be achieved (in terms of channel capacity at given SNR) can be evaluated as:

$$C_{MIMO} = E_H \left[\max_{Q:Tr(Q)=P} \log_2 \det\left(I_N + \rho H_f \times Q \times H_f^{H}\right) \right]$$

$$= E_H \left[\max_{\alpha i:\sum_{1}^{N} \alpha i = M} \sum_{i=1}^{N} \log_2\left(1 + \rho_i(\alpha_i)\lambda_i^2\right) \right] \text{[bit/s/Hz]}$$

Where:

$$\rho = \frac{\alpha_i P}{N_{0,i}B} = \text{SNR of the i-th MIMO sub-channel}$$

P   = Total Transmission Power Level [W]

$N_{0,i}$ = Noise Power Spectral Density of the i-th MIMO sub-channel [W/Hz]

B   = Bandwidth [Hz]

αi   = Transmission Power Weight i-th MIMO transmitter (for Water Filling/Pouring Algorithm)

λ_i^2 = Singular Value (Eigenvalue) related to the i-th MIMO sub-channel for the product matrix $\mathbf{H_f} \times \mathbf{H_f^{H}}$.

The above formula stands when the channel is in same way known in RX section and when the transmission power is allocated in the more suitable way according to the MIMO sub-channel conditions. This optimal power allocation is known as "Water Filling/Pouring" algorithm.

Thus α_i weights can be chosen according to:

$\alpha_i^* = \text{argmax}|_{\alpha i} \{ \Sigma_{i=1,...N} \log_2\{1+\rho_i(\alpha_i)\lambda_i\} \text{ and } \Sigma_{i=1,...N} \{\alpha_i\} = M \rightarrow$ **Water Filling/Pouring**

In case that the channel is known but no optimal power allocation is implemented than the most reasonable solution is to share the total transmission power (P) between all the MIMO transmitters (uniform way). So the Capacity formula becomes

$$C_{MIMO} = E_H \left[\log_2 \det\left(I_N + \frac{P}{M} H_f \times H_f^{H} \right) \right] \text{[bit/s/Hz]}$$

Thus α_i weights can be chosen according to:

$\alpha_1 = \alpha_2 = \ldots = \alpha_N = 1/M \rightarrow$ **no power optimization** (the same SISO transmission power level is split between all the MIMO sub-channels)

Both formulas above are the generalized form of the well-known Shannon-Hartley formula. It represents the theoretical upper limit for the capacity of any band-limited MIMO channel, which cannot be over-performed.

The capacity limit "C" value depends also on the channel matrix "$\mathbf{H_f}$". This is a major difference with respect to the original Shannon-Hartley formulation for SISO systems, because it introduces the concept that the channel structure affects the performance of the system.

In order to compare the performance in term of capacity between SISO and MIMO systems, a "Capacity Gain" parameter is defined as:

$$Capacity\_Gain = \frac{C_{MIMO}}{C_{SISO}}$$

Where the symbols C_{SISO} and C_{MIMO} are defined in the present clause.

In figure 4.4.a and figure 4.4.b the Capacity Gain for a 2×2 MIMO system are reported in the two case of power constraint (i.e. $\alpha_1=\alpha_2=1/2$) and no power constraint ($\alpha_1=\alpha_2=1$). Also the correspondent SNR gain plots are shown for both cases as references.
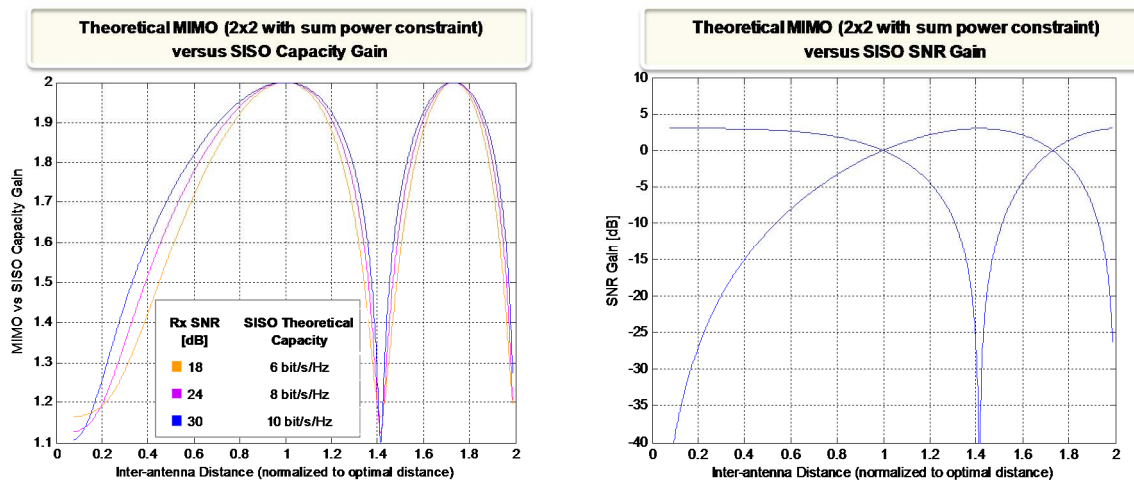
**Figure 4.4.a: Capacity Gain 2 × 2 MIMO with sum power constrain (left)
and SNR Gain with sum power constrain (right)**
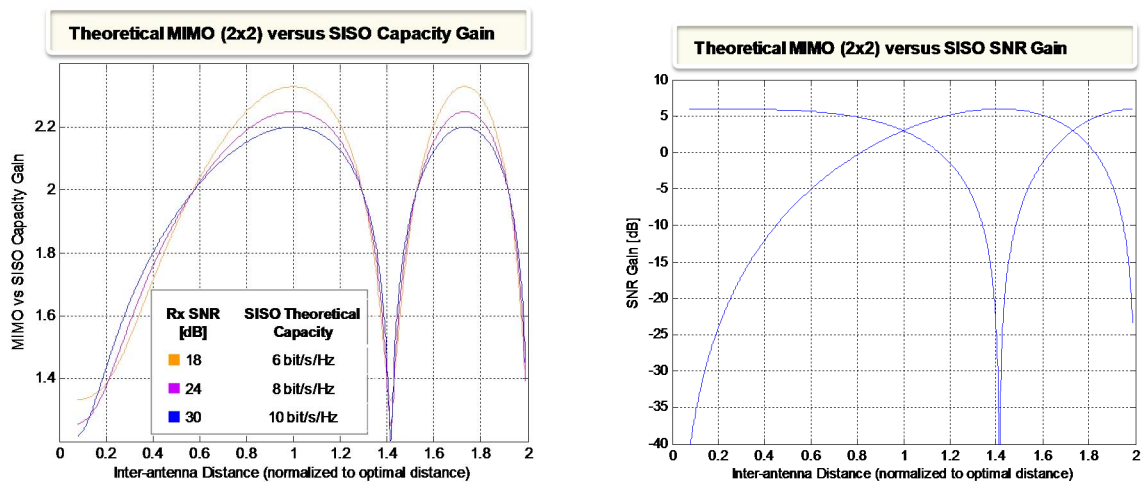
**Figure 4.4.b: Capacity Gain 2 × 2 MIMO without sum power constrain (left)
and SNR Gain without sum power (right)**

It should be highlighted the fact that in case of no power constrain the Capacity gain results higher than 2 (twice), or in general N-times, the SISO Capacity at optimal separation distance between antennas. This is relevant for MIMO link planning for its impact on the maximum licensed E.I.R.P.

4.5   The spatial frequency reuse canceller

4.5.1   Open-Loop MIMO

When the channel is unknown as in open-loop MIMO, the spatial frequency reuse canceller try to suppress the mutual-interference that comes from the "M" TX sub-channels from the useful sub-channel at each of the "N" receiver. These kinds of techniques are similar to ones used by "traditional" interference suppression in equalizers.

- **Optimum Decoding: Maximum-Likelihood (ML) Detection**

    The optimum decoder is the maximum-likelihood decoder. It finds the most likely transmitted vector "**y**" by minimizing the distance:

$$\bar{y} = \operatorname{argmin}\left\|\bar{r} - H \times \bar{y}\right\|^2$$

The main disadvantage of ML detector algorithm is the complexity which is proportional to "m^M", where m is the modulation order and M is the number of transmitter antennas.

Anyway sub-optimal techniques, which reduce the complexity, were developed.

- **Linear Detectors**

  It is possibly the simplest algorithm available. The most common version is the **Zero-Forcing Detector (ZF)**, which sets the receiver filter to the inverse of the estimated channel matrix and removes the mutual interference. This technique is very sensitive to the "nature" of the channel matrix "**H**" as, in case of "bad" sub-channels the noise, "**n**", can be amplified.

  A valuable alternative is the **MMSE Detector** which in the suppression of the interference also minimizes the distortion thus limiting the noise enhancement.

- **Interference cancellation: BLAST**

  In order to improve the performance of decoding algorithm, recursive technique can be used. **Bell Laboratories Layered Space Time (BLAST)** is based on a sequence of steps and iterations. Received signal with best SNR and lowest interference in the input signal is decoded first (this is the "s_1" signal). The recovered "s_1" signal is then erased from the input (combined) received signal. The decoding algorithm is applied again to the (erased) transmitted signal with best SNR and lowest interference (remember that the "s_1" signal, which was the strongest auto-interferer for the other signals, has been erased) then "s_2" signal is decoded.

  Both the recovered "s_1" and "s_2" signals can now be erased from the input (combined) received signal.

  The decoding algorithm is applied again to the (erased) transmitted signal with best SNR and lowest interference (remember that the "s_1" and "s_2" signals, which were the strongest auto-interferers, have been erased) then "s_3" signal is decoded.

  The process is iterated until "s_N" is finally decoded.

  Any basic MIMO decoding algorithm can be used in principle: ML, ZF, MMSE, etc. Thus: Minimum Mean Squared Error - VBLAST (MMSE - VBLAST) if MMSE root decoding algorithm is used or Zero Forcing - VBLAST (ZF - VBLAST) if ZF root decoding algorithm is used.

4.5.2   Closed-Loop MIMO

In closed-loop MIMO some information related to the estimated channel is fed back from the RX to the TX.

In order to reduce the information volume a quantized version of the channel state information is provided to the transmitter (figure 4.5.2.a). Many different algorithms for closed-loop MIMO were presented which require according to their nature a complete or partial channel knowledge.
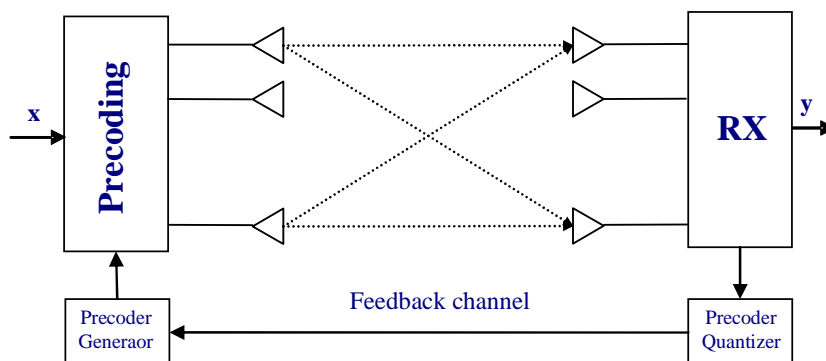

Figure 4.5.2.a: Closed-Loop MIMO

Singular-Value Decomposition (SVD)

The MIMO channel matrix can be decomposed via the singular value decomposition (SVD):

$$H = U \times \Sigma \times V^H$$

Where "U" and "V" are unitary matrices, i.e., $U \times U^H = I$, and $V \times V^H = I$.

The matrix "D" is diagonal and contains the singular values of "H", which are the (positive) square roots of the eigenvalues of $H \times H^H$ and $H^H \times H$.

The MIMO model equations can be written as:

$$y(t) = H(t)x(t) + n(t)$$

Thus:

$$y(t) = U \times \Sigma \times V^H x(t) + n(t)$$

This means that in TX side the transmitted symbols are multiplied by matrix "V". The elements of matrix "V", used by Precoding, is expected to be feed back to the TX by the RX:

$$x'(t) = Vx(t)$$

In RX the signals are multiplied by matrix "U^H", Postcoding operation:

$$U^H y'(t) = U^H \left(U \times \Sigma \times V^H x'(t) + n(t) \right) =$$
$$= \Sigma x(t) + U^H n(t) =$$
$$= y(t)$$

The diagonalization operation is equivalent to remove all the spatial interference without any matrix inversions or non-linear processing. The final result is to break up the MIMO channel in "N" Gaussian sub-channels. This approach is illustrated in figure 4.5.2.b.

SVD does not enhance noise because the matrix "U" is unitary and the product matrix "$U \times Hn$" still has the same variance of "n".

The common drawback for closed-loop MIMO is that the channel matrix "H" needs to be known at both the transmitter and the receiver so the SVD can be computed.
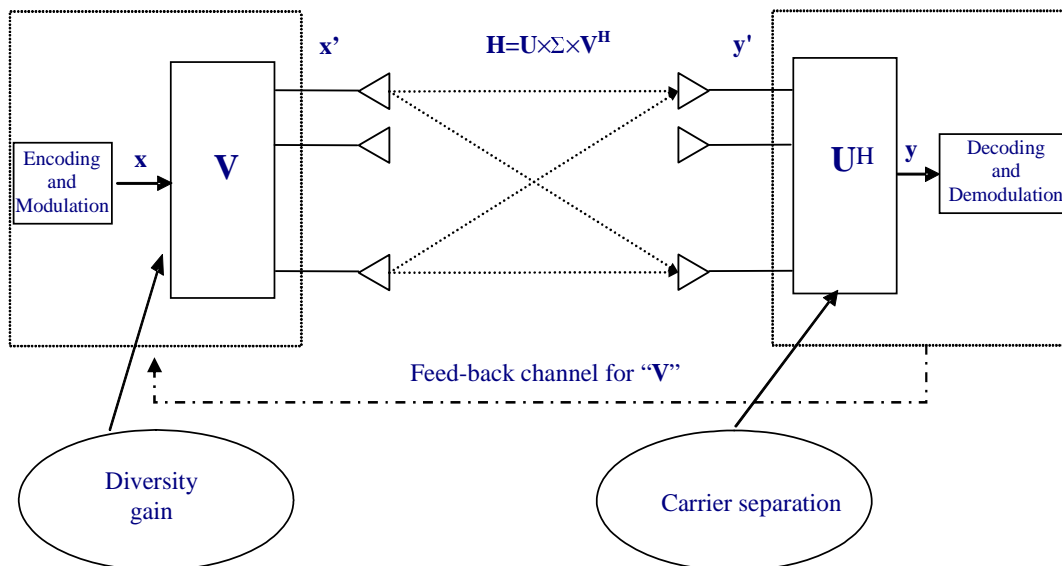

Figure 4.5.2.b: The SVD link presentation

Linear Precoding and Postcoding

Generally the precoder and the postcoder operations can be jointly designed in order either to increase capacity or improve availability or SNR at RX side.

Despite the design criteria the scope of the precoding and postcoding is to decompose the MIMO channel in to a set of "independent" sub-channels as shown in figure 4.5.2.c.
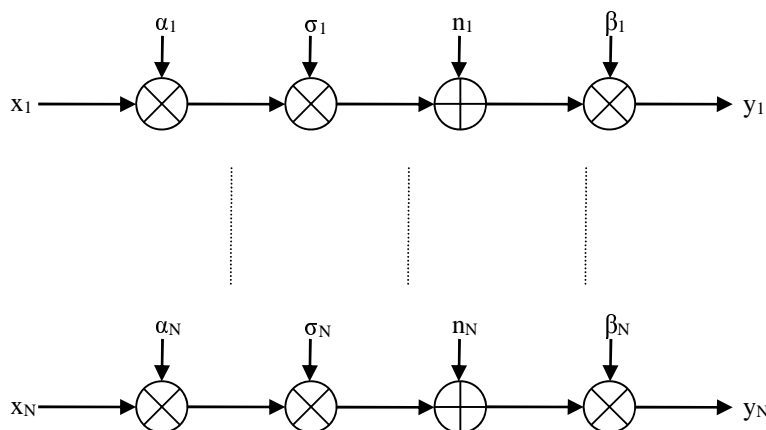

Figure 4.5.2.c: Sub-channels resulting from precoding and postcoding operations

The receiver symbol for the i-th sub-channel is:

$$y_i = \alpha_i \times \sigma_i \times \beta_i \times x_i + \beta_i \times n_i, \, \text{i} = 1, \dots N$$

Where "x_i" and "y_i" are, as usual, the transmitted and received symbols, "σ_i" is the singular value of the channel matrix "$\mathbf{H}$" and "α_i" and "β_i" are respectively the precoder and the postcoder weights.

By using the precoding weights, the precoder can increase the capacity by setting higher transmission power to sub-channels with higher gains and less to the others (Water Filling/Pouring). This is the ultimate reason of the capacity gain of the linear precoding over open-loop MIMO (e.g. BLAST).

4.5.3   MIMO receiver cancellation technique comparison

Following figure 4.5.3 shows Capacity Gain versus Inter-antenna Distance slope when different receiver cancellation techniques are used:

1)   Blue curve: all the four MIMO sub-channels have the same spectrum efficiency and the transmission power is allocated uniformly between the sub-channels. The receiver algorithm is the MMSE detector one.

2)   Yellow curve: theoretical maximum, the spectrum efficiency of the four MIMO sub-channels are not allocated uniformly and also the transmission power is not allocated uniformly between the sub-channels (Water Filling/Pouring). The receiver algorithm is the SVD one.

Theoretical MIMO (Dual Pol 2x2) versus SISO Capacity Gain
@ SNR = 24 dB (8 bit/s/Hz SISO Theoretical Capacity)

Non-uniform capacity among streams

Uniform capacity among streams

MIMO vs SISO Capacity Gain

Maximum Theoretical (Optimal powers)
Linear MIMO Receiver (Equal Powers)

Inter-antenna Distance (normalized to optimal distance)

Notice: Sum power constraint is $2P$, where P is the SISO output power

Figure 4.5.3: Capacity Gain versus Antenna Distance using different MIMO algorithms

It is possible to notice that the MIMO performances are sensitive to the actual spatial frequency reuse canceller algorithm used. Even moving from the ideally condition of maximum orthogonality, d_{opt}, the capacity dropt may be damped by using proper algorithm strategy.

5   Verification by field trial and simulation

5.1   Overview

In order to verify the above described theoretical claims two field tests are presented:

- A 5 GHz field trial. It was implemented by using generic test equipment at 5,8 GHz in urban environment scenario.

- An 18 GHz field trial. It was performed by using its own 18 GHz MW equipment with a new MIMO Modem board in LOS propagation condition.

5.2   5 GHz field trial

5.2.1   MIMO channel measurement experiment - Aims

Measurement of the steady state after settling of multipath transient, in single frequency of 5,8 GHz the complex (amplitude and phase) channel transfer function matrix (four inputs, four outputs) of a spatial 4×4 MIMO channel. It was decided to select low frequency in order to evaluate the scattered channel model and its contribution to the capacity.

Measurement of the channel frequency response:

- Wide band   5,67 GHz to 5,85 GHz (180 MHz).

- Narrow band   5,8 GHz to 5,808 GHz (8 MHz).

5.2.2   MIMO channel measurement experiment - Configuration and plan

Antenna configurations:

- Linear array - four evenly spaced antennas - vertical and horizontal polarizations;

- Element spacing - close (30 cm) to wide (greater than 3 m).

In order to perform the test a special test setup was built. The test was conducted in four different terrains. As an accessory to the trial a special van with 20 metre crane was used in order to be able to do the tests indifferent sites and different heights of the antennas.

Considered topography:

- LOS.

- NLOS.

- Indoor - 7 m distance.

- Short link range (from 500 m to 800 m) window to roof, roof to roof and roof to van.

- Long range - 5 km roof to roof (city centre) and roof to crane (low buildings and scattered high buildings).

5.2.3   MIMO channel measurement setup

5.2.3.1   Tx setup

Figure 5.2.3.1 describes the TX setup which comprises: sweeper synthesized source, power amplifier RF switch and four horn antennas. A special switch controller commutate between the four antenna such that only one antenna transmitted in a certain instant.

Furthermore one of the switch state is "mute - no transmitting". This state was planned to synchronize the RX site to the antenna commutator.
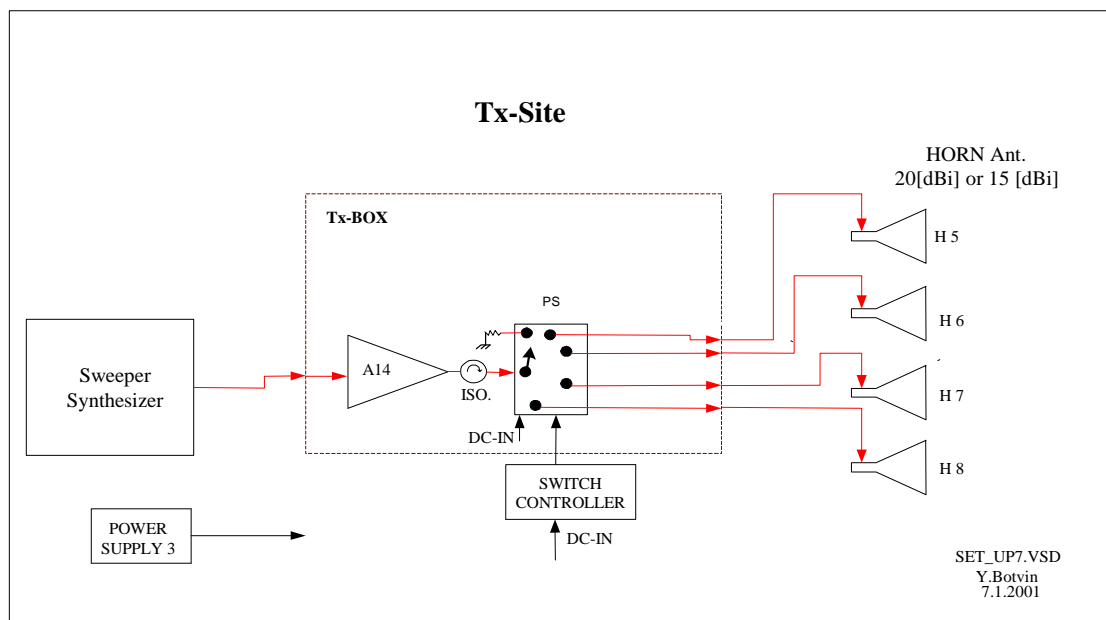

Figure 5.2.3.1: TX site test setup

5.2.3.2   RX setup

Figure 5.2.3.2 describes the RX setup which comprises: two network analysers that act as four channel complex (amplitude and phase) receivers, synthesizer as local oscillator and quad-channel RF front-end. All four receiver inputs operate in parallel.
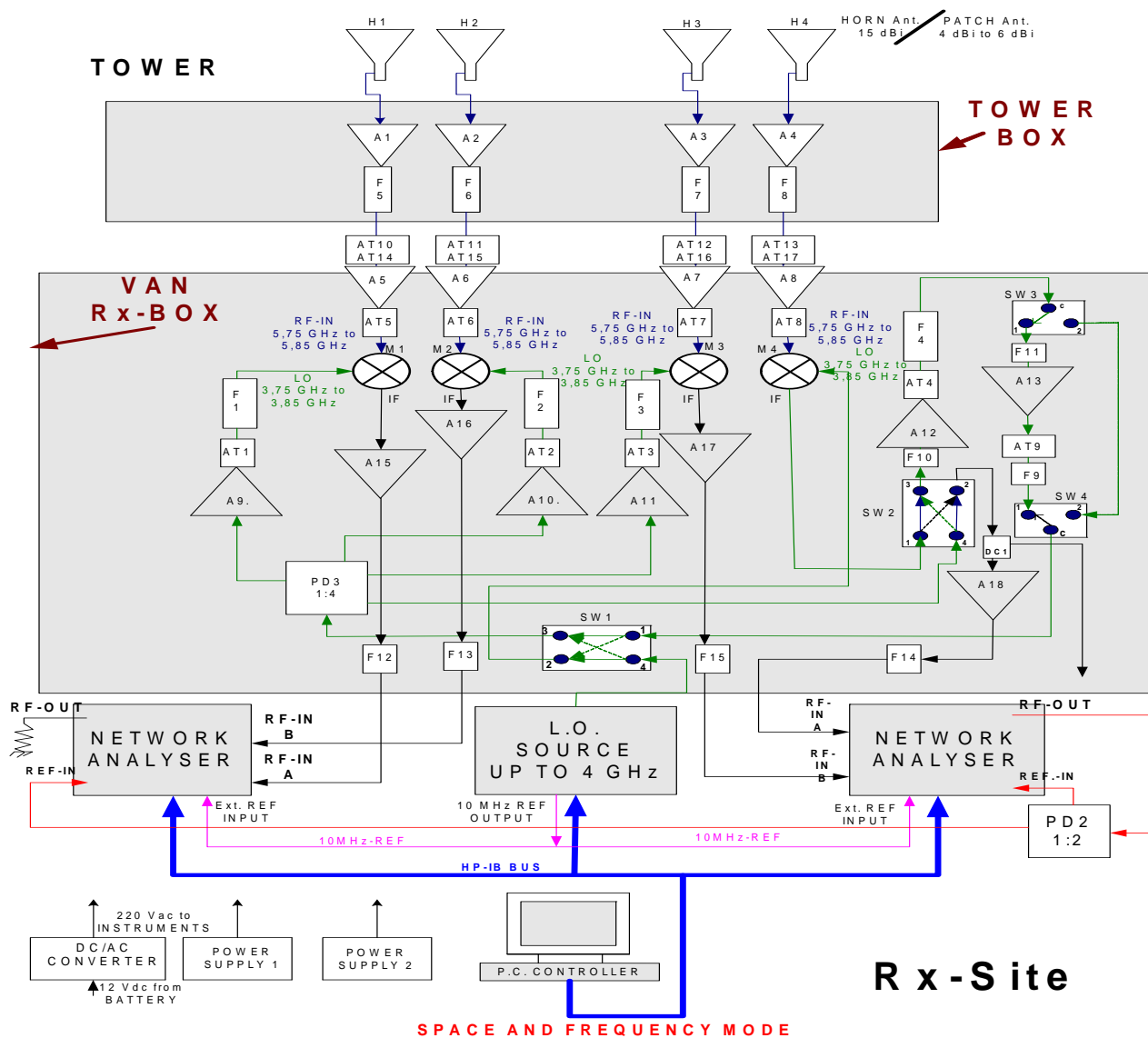
Figure 5.2.3.2: RX site test setup

5.2.3.3   Test results and analysis

5.2.3.3.1   Results

In order to verify the spatial frequency reuse performance the main figures of merit were the four normalized singular values of the channel. The test was conducted between two windows of two different building with 700 m distance. Table 5.1.3.3.1 holds the singular values results of the different tests. Every test was conducted repeatedly with varying antenna spacing.

Test details:

- Singular value test.

- RX-TX spacing: 700 m.

- Antenna Position: horizontal.

- Polarization: vertical.

Table 5.2.3.3.1: Resulted singular values in geometrical spatial frequency reuse

Antenna spacing 250 cm				
Test file name_	Normalized singular values			
BATM_4_SV_test_030601161243	2,452	2,1691	1,7154	1,5298
BATM_4_SV_test_030601161255	2,4497	2,1715	1,7241	1,5202
BATM_4_SV_test_030601161454	2,4497	2,1671	1,7166	1,5349
BATM_4_SV_test_030601161505	2,4488	2,1628	1,72	1,5386
BATM_4_SV_test_030601161516	2,4452	2,1698	1,7198	1,5346

Antenna spacing 200 cm				
Test file name_	Normalized singular values			
BATM_4_SV_test_030601142729	2,917	2,095	1,6531	0,60771
BATM_4_SV_test_030601142806	2,9093	2,1009	1,6617	0,6008
BATM_4_SV_test_030601142817	2,9247	2,0916	1,6479	0,59672

Antenna spacing 150 cm				
Test file name_	Normalized singular values			
BATM_4_SV_test_030601164553	3,1931	2,0857	1,0776	0,54081
BATM_4_SV_test_030601164629	2,9815	2,2911	1,3436	0,23703
BATM_4_SV_test_030601164643	2,9801	2,2852	1,3552	0,24624
BATM_4_SV_test_030601164656	2,9782	2,293	1,348	0,23579

Antenna spacing 100 cm				
Test file name_	Normalized singular values			
BATM_4_SV_test_030601170801	3,6943	1,5111	0,25797	0,04664
BATM_4_SV_test_030601170905	3,6995	1,4999	0,24939	0,040236

5.2.3.3.2   Analysis

From the values in table 5.2.3.3.1.a it can be concluded that the singular values dependence on the antenna spacing can be evaluated and drawn in figure 5.2.3.3.2.a, which depicts the theoretical dependence comparable to the trial resulted dependence. The channel impulse response, reported in the four charts of figure 5.2.3.3.2.b, go toward convergence to the same theoretical point and the matching to the theoretical case is well accepted. The differences exist mainly because of heavy multipath experienced at 5,8 GHz as it can be viewed from the channel transfer function and the impulse response.

If the trial had been conducted in a higher frequency band, where the multipath energy is lower, the matching to the theoretical case would have been even better. It can be viewed also that multipath scattering is flattening the singular value even with lower than optimal antenna spacing, a phenomena that has been exploited in the scattering based spatial frequency system.
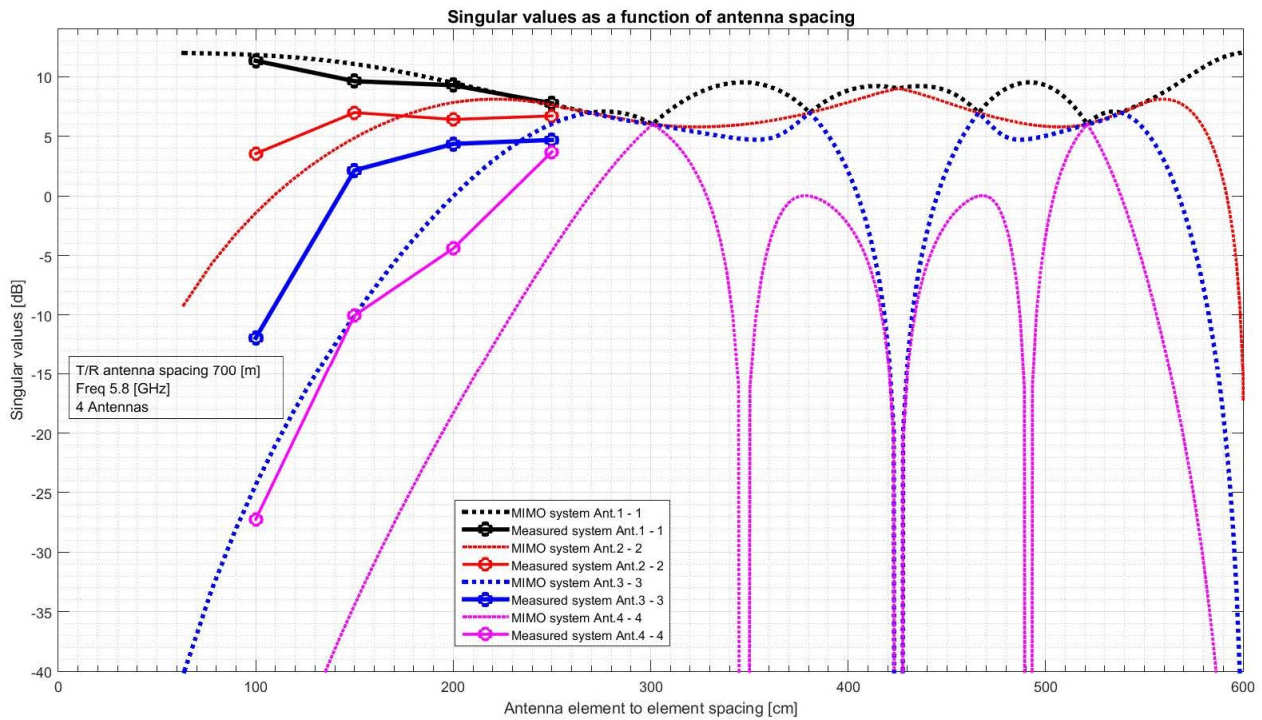
Figure 5.2.3.3.2.a: Analysis of resulted singular values in geometric spatial frequency reuse
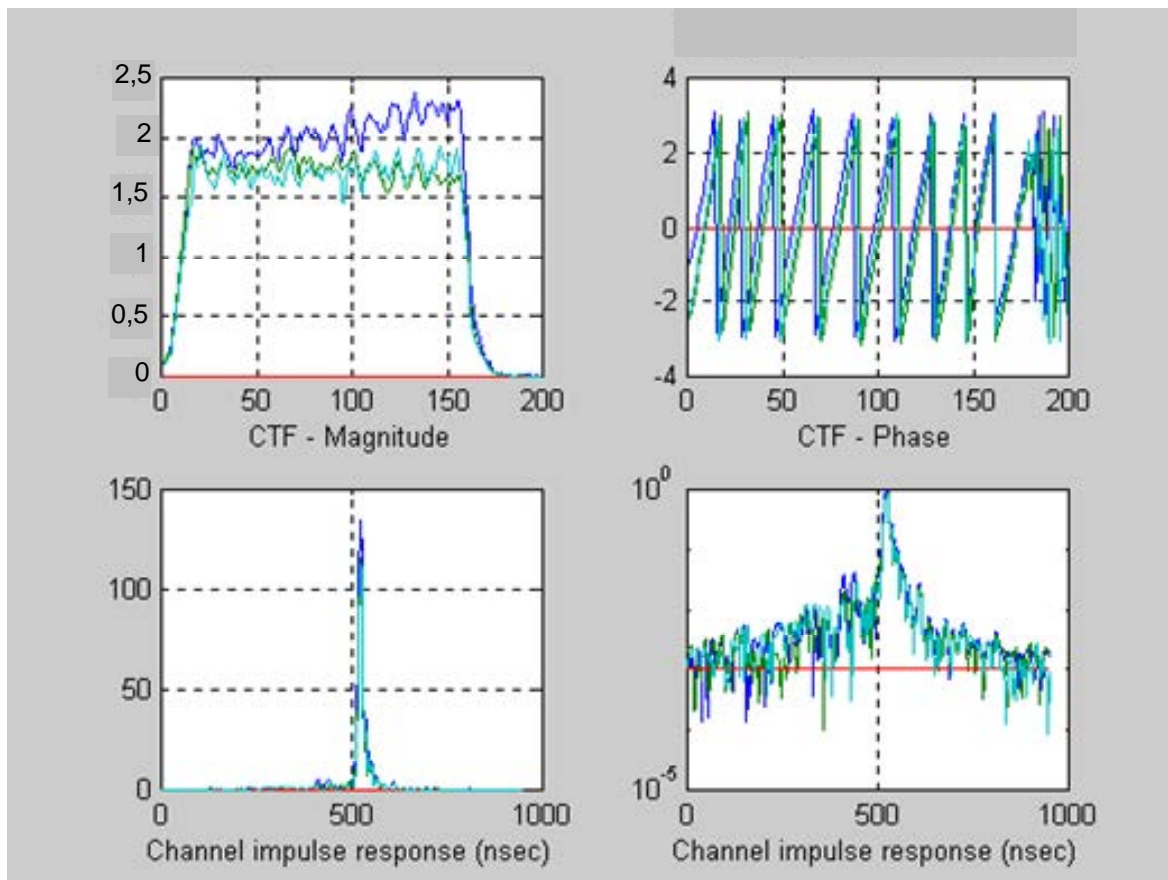

Figure 5.2.3.3.2.b: Channel transfer function in frequency and time domain

5.2.3.3.3   MIMO channel measurement experiment - Conclusions

- Geometric separation of antennas always works according to theory.

    - Line-of-Sight yields low propagation loss.

    - Line-of-Sight yields "static" channel parameters.

- Difficult to find reflections with energies comparable to Line-of-Sight condition.

    - Moderate singular value spread even with some reflections.

    - Low singular value spread obtained by going below the horizon pays dearly in path loss.

    - Low singular value spread obtained by positioning antennas to obtain reflections from large objects, has moderate (15 dB) path loss relative to line of sight.

5.3   18 GHz field trial

5.3.1   MIMO channel measurement experiment - Aims

A MIMO trial was set and tested in order to analyze Multi-Polarized 2×2 MIMO in LOS channel without any power constraint (the MIMO transmission power is double with respect to the SISO one). The selected carrier frequency is 18 GHz with CS = 55 MHz and the modulation format is 256-QAM. The frequency band was chosen due to the availability of an existing experimental SISO link which was upgraded to MIMO saving the installation of one of the two required dual-polarized antennas.

One of the main scopes of the experimentation was to increase the link capacity according to the MIMO theory.

5.3.2   MIMO channel measurement experiment - Configuration and plan

The optimal antenna distance (d_{opt}), over a 6,2 km link hop length, is 7,1 m but for practical installation matter it was only possible to install antennas with 4,3 m of separation. The last value corresponds to the 60 % of the optimal distance and it drives to around 4,5 dB drop in SNR gain.

The MIMO configuration is 2×2 plus CCDP arrangement, thus four sub-channels were achieved.

Site A

6.05 km

Site B

INSTALLATION(*)

Site Name	Site Type	Distance (Km)
A	Hub	-
B	Remote	6.05

(*) Positions have been calculated with GPS and used as referred value for the trial

LINK CONFIGURATION

Site Name	Band	Freq. TX	Channel	Mod.	PTx	AM	ATPC	Antennas	Sys. Cfg.	Antennas distance	Throughput
A	18GHz	18.751.250	55MHz	256QAM	15dBm	OFF	OFF	60cm	2x2MIMO + XPIC	4.3m = 60% Dopt (7.1m)	1.4Gbps
B	18GHz	17.441.250	55MHz	256QAM	15dBm	OFF	OFF	60cm	2x2MIMO + XPIC	4.3m	1.4Gbps

LINK PLANNING(**)

RSL planned (dBm)	Availability H (%)	Availability V (%)
-45.9	99,9939	99,9965

(**) Link planning has been performed using traditional XPIC configuration and without considering MIMO degradation

Expected degradation respect to Dopt

| SNR gain @60% Dopt |
|--------------------|
| -4.5dB |

Figure 5.3.2: MIMO link details

5.3.3   MIMO channel measurement setup

In figure 5.3.3 a sketch of the used MIMO setup is presented. It comprises eight commercial ODUs and two IDUs with a new MIMO modem board, four dual-polarized 60 cm diameter dish antennas, a traffic generator/analyzer instrument, a data logger, a weather station meter and laptop for controlling the link.
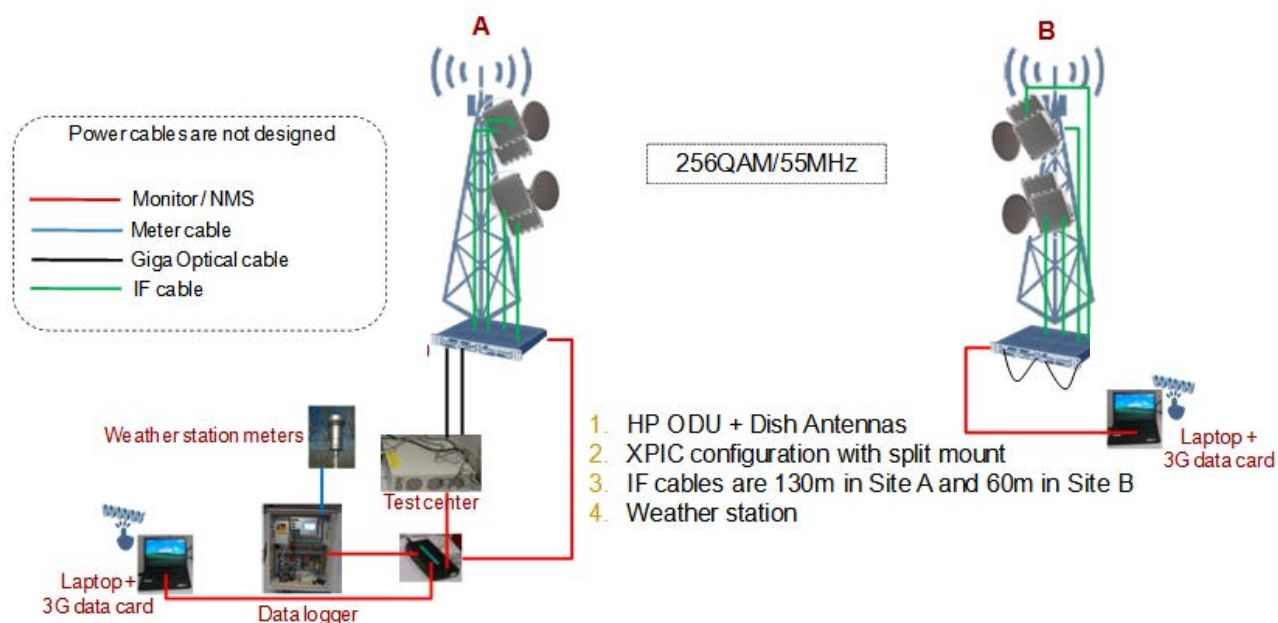
Figure 5.3.3: MIMO link layout

5.3.4   Test results and analysis

In the three layers of figure 5.3.4 are shown:

- **The RSL values for the four MIMO sub-channel in one direction.**

  Due to many tolerance sources in the link setup the RSL values are not at the same level, anyway the RSL values for links with the same polarization are kept in a reasonable ± 3 dB spread.

- **The MSE (SNR) values at RX side for the four MIMO sub-channel in one direction.**

  For the four sub-channels the MSE evolutions are very irregular with an average of 32 dB.

- **The whole MIMO capacity.**

  The resulting capacity measured was around 1,4 Gbit/s and it was quite stable during the recording time.

  Considering that an average throughput for a SISO 256-QAM over 55 MHz CS configuration is around 410 Mbit/s, 3,4 times the SISO capacity using MIMO configuration was achieved.

These results are a subset of the measurements performed during the experimental period, in particular just seven days record is reported.

Figure 5.3.4: RSL, MSE and Capacity results

6   Verification by simulation

6.1   The simulation block diagram

As an additional engine to the trial verification at 5 GHz, in order to verify the spatial frequency reuse theory, to learn about sensitivities and to evaluate the performance a special simulation was developed. Another goal of the simulation was to develop algorithms of SFRC and to assist with the implementation phase. Figure 6.1.a describes the top level simulation of the four spatial channels. Figures 6.1.b, figure 6.1.c and figure 6.1.d describe the simulation main parts: modulator, channel and demodulator. The simulation assumes narrow.band QAM signal with added Gaussian noise, phase noise channel multipath and frequency/timing mismatch.
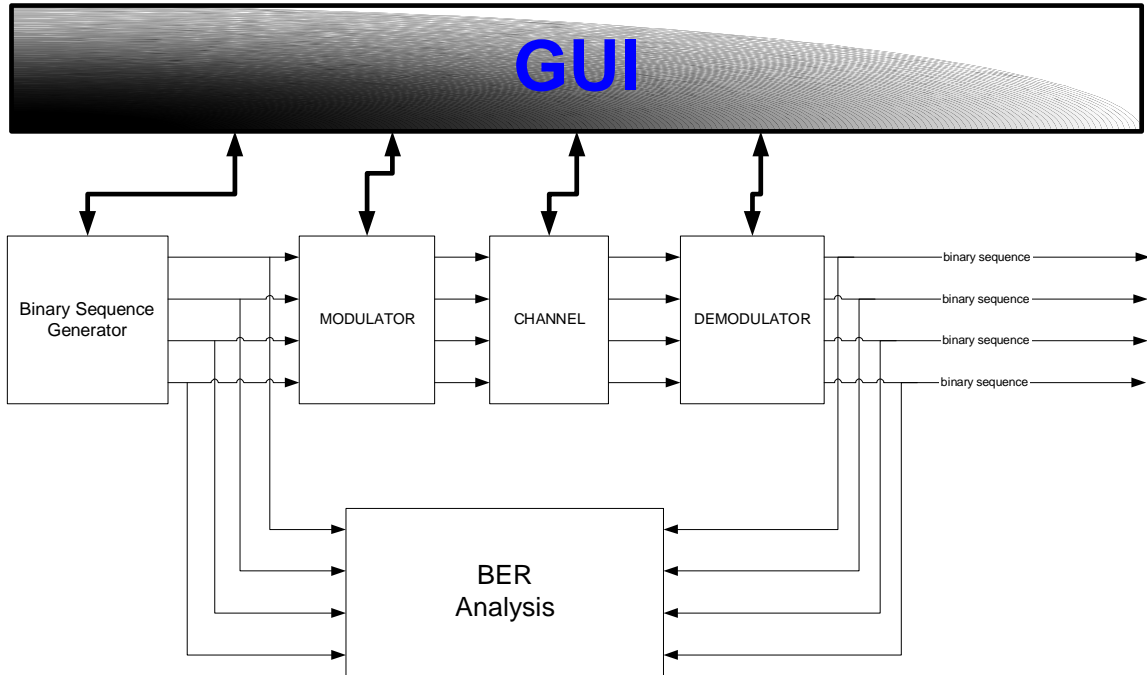
**Figure 6.1.a: Simulation top-level block diagram**
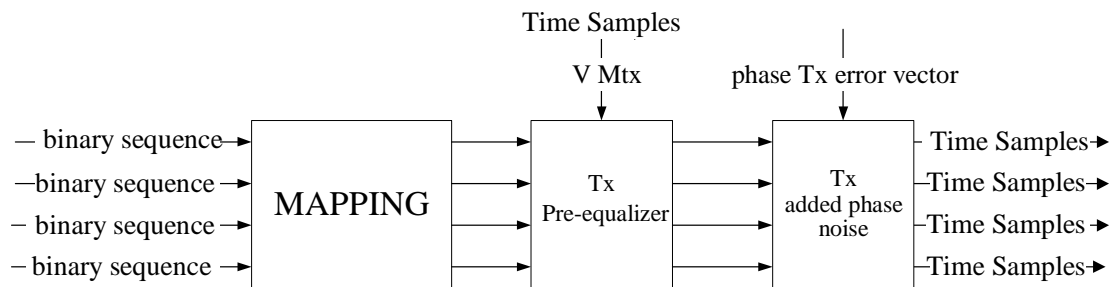

Figure 6.1.b: Modulator simulation
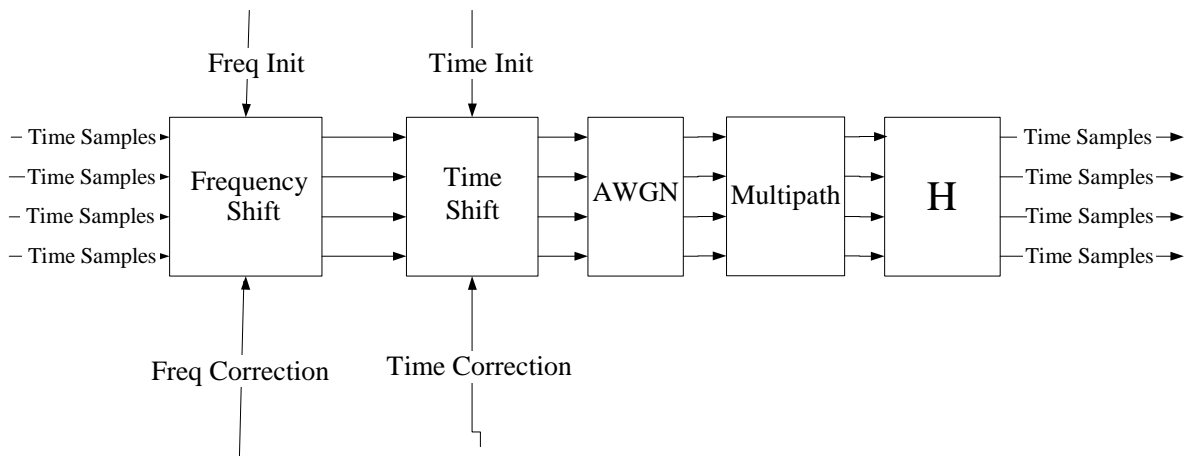

Figure 6.1.c: Channel simulation
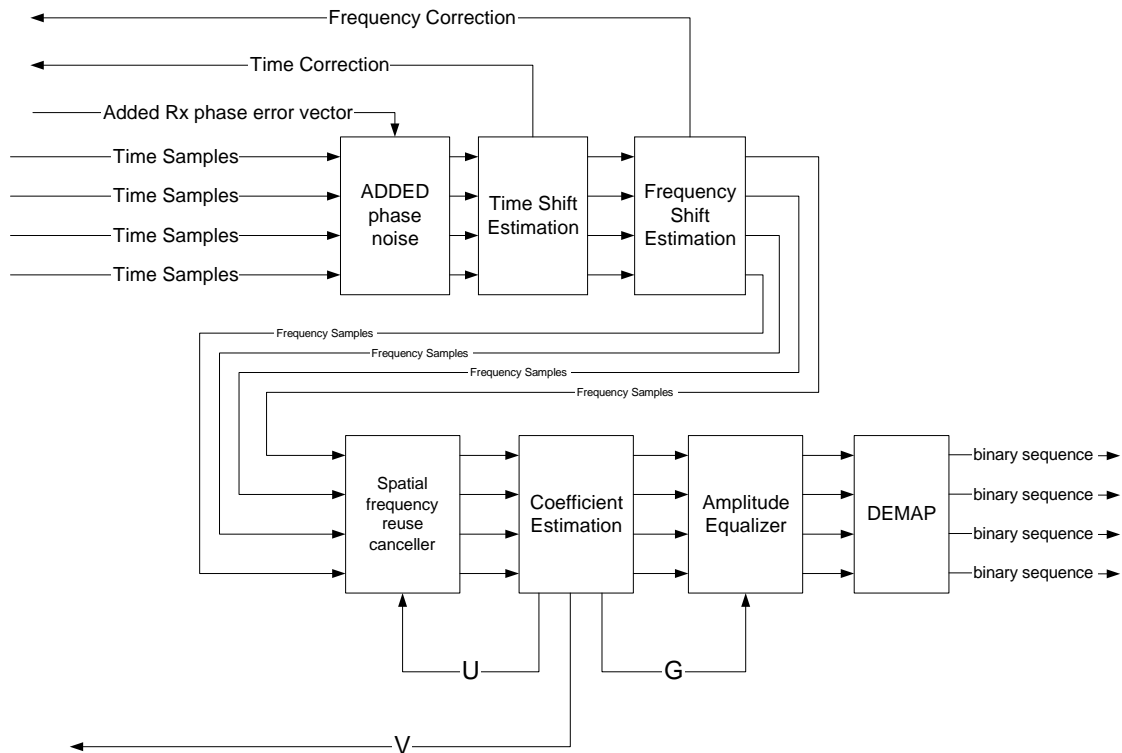
Figure 6.1.d: Demodulator simulation

6.2 The simulation results

Table 6.2 summarizes the results for few variations of multipath scattering and spatial phase noise of TX and RX performances by measuring C/N ratio at the detector.

Table 6.2: Resulted singular values in geometrical spatial frequency reuse

Digital Modulation: **128 QAM**					
Analog Modulation: **Fs/4, SAW filter**					
Self Noise level: **-41,8 dB**					
External Noise Level: **-Inf** (no noise added)					
MP Angles degrees	**Phase mean (°)**	**Phase STD (°)**	**-20 dB @ 8 ns (dB)**	**-15 dB @ 16 ns (dB)**	**-15 dB @ 8 ns (dB)**
Tx = [1,5, -1] Rx = [-0,5, -2]	-0,5	1,47	41,5	37,6	38
Tx = [3, -2] Rx = [-1, -4]	-1	2,94	34,1	N.A.	N.A.
Tx = [-2,9, -14] Rx = [-3,1, 6,2]	0,0197	4,34	33,8	32,3	31

7 Void

Void.

8 Practical implementation

8.1 Overview

Similar to the implementation of the XPIC, the SFRC can be implemented with split-mount architecture with separate ODUs which are tied together with the IDU (see figure 5.3.3). ODUs should be synchronized together in the symbol timing and the reference source to the local oscillators that form the carrier frequency. At the base-band interface there should be a mux/demux mechanism that distributes the payload at the input the transmitter and aggregates it back out of the receiver.

8.2 Installation Issues

Out of the antenna spacing and orientation, there is no any special requirements for the installation of MIMO system. The installation is very much similar to a conventional PP link; each antenna direction can be adjusted separately according to line of the antenna array.

In figure 8.2.a and figure 8.2.b the simulation results of effect of antenna misalignments are reported in the case of "theoretical" (closed-loop MIMO) and linear MMSE MIMO receiver types.
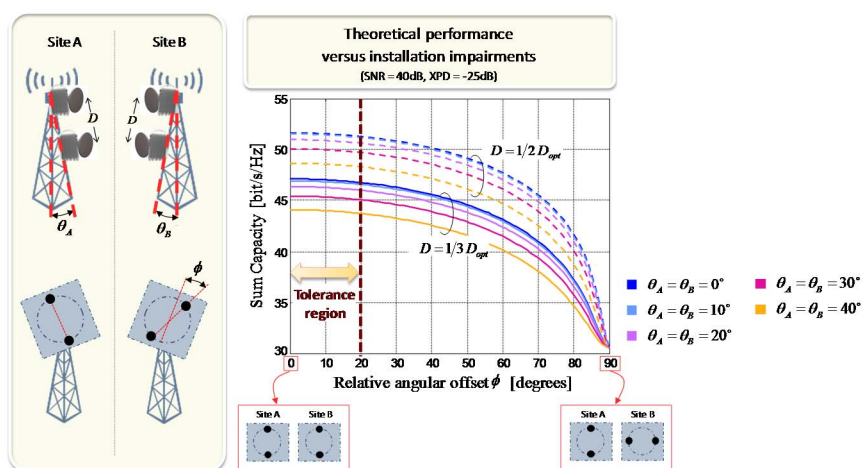

Figure 8.2.a: Installation impairments with theoretical receiver performance
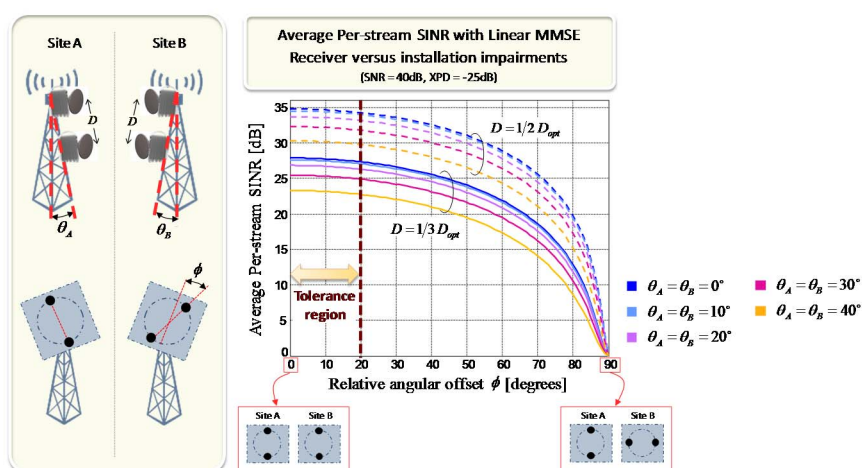

Figure 8.2.b: Installation impairments with linear MMSE receiver performance

8.3   Availability Calculation

The MIMO link availability can be expressed by the following formula:

$$Availability = 1 - P\{C_{MIMO}(H_f) < R\} = 1 - P\left\{\left[\log_2 \det\left(I_N + \frac{P}{M}H_f \times H_f^H\right)\right] < R\right\}$$

Where "*R*" is the MIMO data rate [bit/s/Hz] at which the link is designed to work.

The information about the radio channel statistical variations (i.e. the fading attenuation) is accounted for the product term containing the channel matrix (H_f).

At the current stage it is not known the *correlation value* between the fading attenuation faced by each single sub-channel. Thus no availability model can be proposed in a closed form but only simulation can be shown.

(In technical literature some closed availability formulas are provided for well-known fading statistic distributions following Rice and Rayleigh distributions which are usually used to model NLOS Mobile Access radio channel).

For radio links in the frequency bands, where availability is mainly limited by rain attenuation (above 15 GHz), the correlation between each sub-channels can be considered equal to "1". In other words, all the sub-channels fading amplitude values are correlated and thus they assume the same value. In this case the MIMO link availability becomes dependant by the decoding scheme adopted in the receiver.

Furthermore the effect of rain depolarization is expected to be considered in case of multi-polarized MIMO.

9   Summary

Spatial multiplexing is another additional frequency reuse method to the current CCDP one that is suitable for point-to-point application. The present document describes the implementation of the spatial multiplexing in microwave PP equipment which exploits the geometry of the link (i.e. antennas separation) by using MIMO techniques. Such techniques breach the QAM barrier in order to achieve significantly higher spectral efficiencies.

As described in the present document, this technique requires some care in the installation of the PTP link, as antenna alignment, and if the total transmission power level is increased with respect to a SISO link some further performance increase can be reached.

Annex A:
List of Topics to be considered in Standardization

A.1 Topic List

The following topics are proposed to be considered in the framework of managing MIMO configurations:

1) Minimum RIC (Radio Interface Capacity).

   Capacity varies according to MIMO antenna distance. Spectral efficiency may not be uniformly distributed between all MIMO channels to get higher MIMO Overall Capacity.

2) Minimum Received Power Level.

   To be considered +3 dB ($10 \times \log_{10}(M)$, M = MIMO TX antennas) in RSL in case of no power constraint stands.

3) Transmission Power Tolerance (Accuracy).

   The tolerance should consider all the transmitters used in MIMO scheme.

4) Residual BER

   It is necessary to define as the residual BER figure should be tested (e.g. as for CCDP configuration with all the "internal" interference active.

5) Training Sequence.

   It is necessary to interrupt the Traffic to estimate the channel.

6) General Testing Rules.

7) Aligned Harmonized Standard Family with SFR/MIMO definition.

Annex B:
Antenna Geometry and Composite Antenna RPE's

B.1   Antenna Geometry

In the present document only the case of uniform linear array of antenna (ULA) has been considered because it is "easier" to be managed and it corresponds to the tested case in the trial.

However, it is not mandatory to place antennas in straight line and even other antenna array "geometry" can be used. Some examples are uniform rectangular array of antenna (URA) and uniform circular array of antenna (UCA).
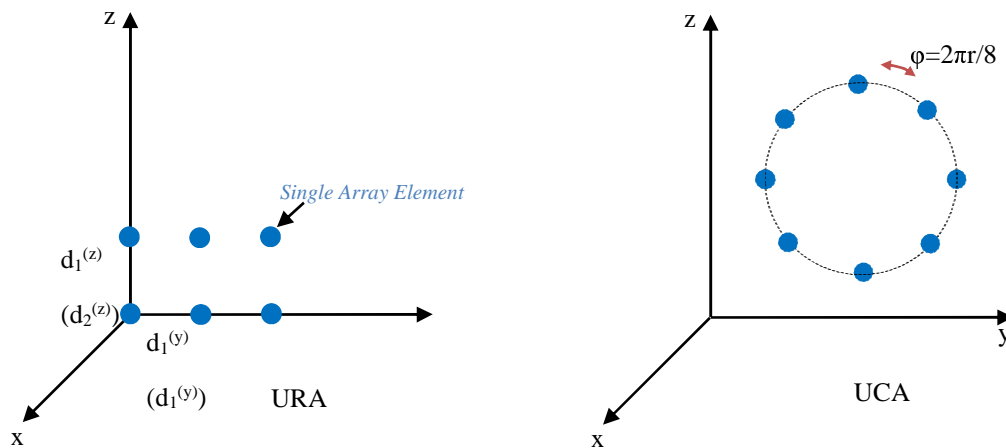

Figure B.1: Antenna geometry examples

The optimal design equations for principal antenna array geometry drives to a formula:

$$d_1\, d_2 = \frac{\lambda\, R}{N\, X}$$

Where "d_1" and "d_2" terms represent the antenna separation values at the two link edges, "R" the hop distance, "N" the number of antennas and the "X" term depends from the orientation of the array and the specific geometry.

The above formula has similar formulation for all the antenna configurations and it is important to highlight that the optimal antenna spacing is directly proportional to the carrier wavelength and the link hop length but it is inversely proportional to the number of antenna.

In any case all the MIMO considerations in the report are valid despite the antenna array geometry used.

B.2   Composite Antenna RPE's

Considering a 2×2 MIMO case, two spatially separated transmitting antennas create gain patterns, i.e. "*Array Factor*", in the far field called grating lobes. For the setup in figure B.2.a below the receiver sees different signal strengths depending on the physical angle φ (for the sake of simplicity only the azimuth plane is considered).
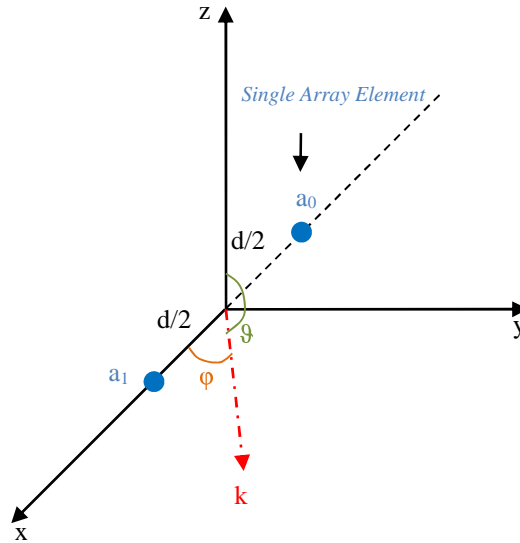
Figure B.2.a: Antenna array example

Array Factor evaluated on the Azimuth ($\vartheta = \pi/2$) plane:

$$A_Z(\phi) = a_0 e^{-j_0 \cdot \frac{d}{2} \cos\phi} + a_1 e^{j_1 \cdot \frac{d}{2} \cos\phi}$$

Where "k_i" (i = 1, 2) is the "Propagation Wavenumber" defined below:

The "*Total Antenna Array Power Gain*" becomes:

$$k = \omega \cdot \sqrt{\mu\varepsilon}$$

$$G_{tot} = |A_Z(\varphi)|^2 \, G(\varphi)$$

Where "$G(\varphi)$" is the single antenna RPE.

For example when using a 2 × 2 MIMO configuration running at 23 GHz of carrier frequency on a link hop length of 5 km, the resulting optimal antenna separation is 5,7 m.

The single antenna RPE has been simulated according to Recommendation ITU-R F.699 [i.1], as in figure B.2.b, and the gain has been normalized in order to result in 0 dB (the absolute gain is 41 dB as a 60 cm diameter antenna has been chosen).
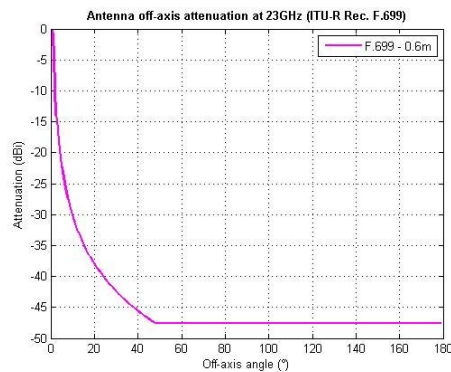

Figure B.2.b: Recommendation ITU-R F.699 [i.1] Antenna RPE

The average on time total antenna array power gain ("G_{tot}") is depicted by the blue envelope in figure B.2.c and the maximum normalized gain value is 3 dB which represent the sum in power of two non-coherent sources. In fact the two M-QAM signals transmitted by the two antennas are not coherent as phase and also with different amplitudes.

The red envelope represents again the single antenna RPE according to Recommendation ITU-R F.699 [i.1]. The single antenna RPE, "$G(\varphi)$", acts as a spatial filter in the domain of the degree which shapes the final total array RPE.
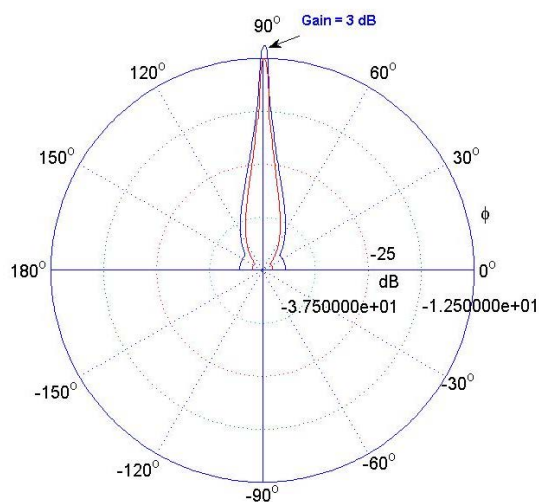
Figure B.2.c: Antenna array power gain (blue envelope) and single antenna RPE (red envelope)

NOTE: As no interference analysis has been performed, only the antenna main radiation lobe has been considered with Recommendation ITU-R F.699 [i.1]. For the same reason also antenna classes have been not mentioned.

Annex C:
MIMO Status in 2014

In year 2014 CEPT Administrations answered to an ECC Questionnaire (7 Questions) related to on MIMO status. Although not all CEPT administrations answered the Questionnaire, some general impressions can be derived and here a short summary of answers is presented for each.

Question 1: Possibility to deploy MIMO technology on licensed Fixed Service point to point links.

13 countries provide a positive answer, 4 do not allow MIMO at the moment but few are considering the issue. Few countries allowing MIMO requests, someone require info an antenna and other are still considering the issue. Potential difficulties of obtaining authorizations for placing multiple antennas have been raised.

Question 2: Need of knowing correct antenna separation to accept the application for licensing.

12 Administrations indicated necessity of having this info available, 7 indicate no need for it and 1 gave no indications. In case the need is indicated, in general it will be subsequently quoted on the granted license.

Question 3: Licensing options.

8 Administrations indicate to licence a whole multi-antenna installation as a single FS stations, 4 indicate to licence each antenna individually by prescribing individual emission parameters for each antenna and 7 indicate they are still considering the issue.

Question 4: Need of executing additional interference analysis because of the two (or more) parallel co-channel transmission paths.

9 Administrations are of the opinion that such analyzes is necessaries and 8 are of opposite view.

Question 5: Possibility to deploy MIMO in all fixed service bands.

8 Administrations allow MIMO use in all frequency bands and 3 indicate limitations for MIMO suitable frequency bands (i.e. above 13 GHz).

Question 6: Charge of a MIMO link compared to a single transmitter link.

About 10 Administration indicate to use the same charge as used for a single link, 5 indicate double charge and 5 are still under decision.

Question 7: Existence of further restrictions to deploy MIMO link (similar to space diversity links).

About 10 Administration indicate that no further restrictions are foreseen, the need of a separate construction permits are indicated by one Administration and the others are still considering the issue.

Comments were given to some answers in particular that few or no requests for MIMO have been received yet by the Administrations. Consequently, at the moment, not all the aspects related to MIMO are well consolidated and they are still under consideration.

History

Document history		
V1.1.1	April 2004	Publication
V1.2.1	November 2015	Publication